RSC Advances

REVIEW

View Article Online
View Journal | View Issue

Cite this: *RSC Adv.*, 2021, **11**, 4375

Biobased foams for thermal insulation: material selection, processing, modelling, and performance

Rebecca Mort,[ac] Keith Vorst,*[bc] Greg Curtzwiler *[bc] and Shan Jiang *[ac]

With the urgent need for the development of sustainable materials and a circular economy, a surge of research regarding biobased materials and associated processing methods has resulted in many experimental biobased foams. Although several biobased foams are already shown to have thermal and mechanical properties competitive with expanded polystyrene, there remains a fundamental knowledge gap leading to limited understanding of the principles that determine performance. This review outlines the progress in this burgeoning field, introducing materials selection and processing, comparing performance, examining efforts in modelling physical properties, and discusses challenges in applying models to real biobased systems. The focus is on low thermal conductivity, which is a critical property for temperature-controlled applications such as packaging for refrigerated/frozen foods, medications, and vaccines as well as building materials. Currently, the trend in the field is moving towards fully biobased and compostable foams, though partially biobased polyurethane foams remain the most consistent performers. To illustrate the foam structure–property relationship, thermal conductivity, cell size, and density data were compiled. Given the complexity of biobased foams, heat transfer models aid in identifying crucial variables. However, data relevant to the insulation capability of biobased foams is not fully reported in many references. To address this issue, we employed a dimensional analysis to fill the gaps, revealing a power law correlation between thermal conductivity and relative density. Our approach is not intended as a robust prediction technique, but rather a simple demonstration of how biobased foams data could be utilized to predict the most promising materials and methods.

Received 31st October 2020
Accepted 9th December 2020

DOI: 10.1039/d0ra09287h

rsc.li/rsc-advances

[a]*Materials Science and Engineering, Iowa State University, Ames, Iowa 50011, USA. E-mail: sjiang1@iastate.edu*

[b]*Food Science and Human Nutrition, Iowa State University, Ames, Iowa 50011, USA*

[c]*Polymer and Food Protection Consortium, Iowa State University, Ames, Iowa 50011, USA*

Rebecca Mort is a second year PhD student at Iowa State University in the department of Materials Science and Engineering and affiliated with the Polymer and Food Protection Consortium. She completed her Bachelor of Science degree in Materials Science and Engineering at Cornell University in 2019. At Iowa State, she is advised by Drs Shan Jiang, Greg Curtzwiler and Keith Vorst. Her current research is focused on sustainable packaging materials and advanced coating technologies.

Dr. Vorst serves as the Director of the Polymer and Food Protection Consortium in the Department of Food Science and Human Nutrition at Iowa State University. Dr Vorst worked in industry for three major packaging companies and served as a consultant for a major automotive manufacturer prior to joining academia in his current position at Iowa State University. Dr Vorst has over 70 publications and 12 published or pending patents for plastics characterization, package design, contamination monitoring, medical device manufacturing, microbial testing methods, and polymer design. Dr Vorst has done extensive work in method development for extractables in packaging materials.

1. Introduction

The growing push towards a more sustainable, circular economy has increased attention on biobased materials that are useful in many applications including coatings, adhesives, medical equipment and single use packaging.[1–4] Besides being more sustainable, multiple studies show that replacing petroleum-based materials with biobased alternatives significantly reduces environmentally harmful emissions.[5–10] Additionally, biobased materials are often biodegradable, thus reducing landfill waste accumulation.[11,12] Development of biobased foams has realized significant advancements in recent years utilizing a multitude of materials and foaming methods. Low thermal conductivity is highly desirable for thermal insulation foams that could be used for packaging and building materials. Several studies have demonstrated biobased or partially biobased foams with thermal conductivity comparable (within 10%) to commercial petroleum-based foams, which are widely used in industry due to their low cost and excellent thermal insulation properties.[13–27] Expanded polystyrene (EPS), commonly referred to by the brand name Styrofoam™, and extruded polystyrene (XPS) are the current standards of foam.

Though petroleum-based foams possess high performance for lightweight, insulating packaging, the materials are highly problematic with regard to sustainability. For example, the production of polystyrene is associated with consumption of non-renewable resources as well as environmentally harmful emissions.[28,29] The foaming process, particularly for extruded foams, has historically contributed to ozone depletion. For example, the use of hydrochlorofluorocarbon (HCFC) blowing agents caused increases in ozone degradation prior to being phased out as mandated by the Clean Air Act and Montreal Protocol.[30,31] Additionally, EPS and XPS products are often disposed in landfills after one-time use rather than recycling. This is in part due to limitations in recycling infrastructure as well as difficulty in shipping and low economic benefit from recovering and recycling polystyrene foams.[32] It is important to note that there has been progress in making recycling EPS more practical. Businesses and governments across the globe are currently increasing their recycling efforts.[33] Along with recycling, finding a more sustainable alternative to EPS/XPS that is comparable in performance is extremely desirable. Given the progress made in recent years, biobased foams have the potential to provide desired properties and eventually replace EPS/XPS.[15,22,23]

Since foaming methods are usually selected based on the raw material, it is critical to understand different processing methods in order to choose the appropriate processing approach and conditions for biobased materials. Foaming methods can be categorized by the blowing agent mechanism: physical or chemical. The blowing agent is a material that rapidly expands inside a polymer melt upon a reduction in pressure.[31,34] Both physical blowing agents (PBAs) and chemical blowing agents (CBAs) are commonly applied to make foams with different mechanical properties. PBAs currently in use are either supercritical fluids (*e.g.* supercritical carbon dioxide) or low boiling point liquids (*e.g.* pentane) introduced and blended directly into a polymer melt.[31,34] CBAs, on the other hand, are solid materials that are added to the polymer melt and decompose to generate dissolved gases during processing. These reactions can be endothermic (*e.g.* citric acid/sodium bicarbonate) or exothermic (*e.g.* azodicarbonamide).[31] PBAs and CBAs both typically require a heated and pressurized vessel such as an extruder, injection mold, or autoclave. Despite similar processing equipment, PBAs and CBAs will typically produce drastically different structures. CBAs often create denser foams and PBAs sometimes result in cell collapse due to oversaturation and fast diffusion.[31,34] In cases for which forming a melt at high pressure is not feasible, a foam structure can be formed through other methods including mixing, phase separation, or a chemical reaction between primary components.[35–37] In some cases, the term "chemical blowing agent" may refer to

Dr. Greg Curtzwiler is an Assistant Professor in the Polymer and Food Protection Consortium at Iowa State University. His research is focused on sustainable materials for adhesives and coatings in the packaging and automotive industries including bio-based, compostable, and recycled polymers. Greg has 21 publications and nine patents to his credit in areas such as food packaging, sustainable polymers, and nanotechnology. He is currently working on understanding the structure–property relationships between polymer structure, water hydrogen bonding, and hydroplasticization of biobased polyesters, polyurethanes, and thiol–ene materials for adhesives and coatings.

Dr. Shan Jiang is an Assistant Professor in the Materials Science and Engineering department at Iowa State University. He obtained his PhD from the University of Illinois at Urbana-Champaign, working with Professor Steve Granick. After graduation, he studied at MIT Langer lab as a postdoc. He then worked for the Dow Chemical Company Coating Materials as a research scientist and a Certified Green Belt Project Leader. Dr Jiang has published more than 50 peer reviewed journal articles and book chapters. He has diverse research interest in both fundamental and applied aspects of soft matter, biomaterials, coatings, and advanced manufacturing.

a reactive component that is not necessarily an independent solid additive. The most typical example of this is using water as a CBA with polyurethane foams, which undergo a chemical reaction induced free rise foaming process. It should be noted this review paper only focuses on foaming methods which produce structurally stable foams. Methods such as Pickering emulsions[38,39] that produce insulating foams with short lifetimes on the order of days or hours are not discussed here.

Biobased foams have been demonstrated with diverse sets of materials, additives, and processing methods, producing structures different from the traditional foam EPS/XPS. Wicklein *et al.*[15] developed anisotropic foams which incorporated graphene nanoparticles to dramatically reduce thermal conductivity in the radial direction. Mihai *et al.*[40] explored the impact of polymer structure on foam crystallinity and resulting density. Qu *et al.*[41] selected a blowing agent specifically to create a disparity between foaming kinetics in the two components of a blend causing a bimodal cell distribution to form. These methods greatly expand the selection of biobased foams. However, the downside of having such wide variety of options is that comparing foam performance and predicting which methods are most promising becomes increasingly complex.

Heat transfer models offer a means to compare and predict foam thermal conductivity. When utilized with knowledge of processing, models can provide insight to how these materials can be manipulated to achieve improved performance. In the majority of cases, convection cannot occur due to gas flow restrictions within closed cells. Therefore, conduction and radiation are generally the main heat transfer mechanisms, but the degree to which they act varies.[42–44] In XPS, conduction accounts for roughly 60–80% of heat transfer while radiation accounts for 20–40%.[43] Thermal conductivity models are able to calculate the contributions of these mechanisms by making assumptions about foam structure and the molecular structure of materials with equations derived from physics of heat transfer.[45,46] Historically, many models have taken a simplified approach to defining structure in order to make separation and analysis of physical variables easier. Wang *et al.* created a model which reduced the structure down to two dimensions and was able to thoroughly examine a large range of average cell sizes and foam void fractions on each heat transfer component.[47] More recent models have increased applicability to less simplified structures. Bernardo *et al.* used parallel and series setups to account for a complete cell size distribution rather than just an average cell size.[48] Though no single model captures the full array of structures displayed by various experimental biobased foams, each model can provide crucial insight into different factors which generally impact thermal performance.

By tuning the assumptions in a model to more accurately reflect materials and processing conditions, models are becoming increasingly effective in fitting and predicting the experimental data. However, even with well-constructed models, there remain gaps in current literature on reported data of thermal conductivity and structure characterization for biobased foams. For example, relative density has been shown to be a reasonably good predictor of thermal conductivity in EPS and polypropylene foams,[26] but is not always reported for biobased foams. Some studies may report apparent density but, as discussed later in this review, these data are insufficient for providing a holistic understanding of foam structure and thermal conductivity. Underreporting thermal conductivity data and critical structural characteristics have created a challenge in validating model performance in predicting properties for biobased systems. Therefore, at the end of this review, we present a new dimensional analysis to fill the data gaps by optimizing fitting parameters. Our mathematical fit is preliminary and not intended to be viewed as a robust model. It does, however, offer a simple means to compare multiple biobased foams datasets to quickly determine which experimental foams are likely to be competitive with EPS. The potential value in applying fitting parameters could be to make heat transfer models more adaptive and representative of real-world scenarios.

This review will first discuss different types of biobased materials used for fabricating foams along with the foaming methods typically employed for each of those materials. The next section will discuss heat transfer modelling in depth by providing background on heat transfer mechanisms and common assumptions and conclusions of various models. The applicability of heat transfer models to biobased foam systems is discussed by comparing the validity of different assumptions and how more recent models derived conclusions which contradict the assumptions of past models. In the last section, thermal conductivity data and structural characteristics of these biobased foams are compiled to identify potential trends present. Finally, a dimensional analysis method is applied to the biobased foam data available in the literature, allowing us to gain a clearer view of trends and to fill in data gaps.

2. Biobased foams

Biobased foams exist in a broad spectrum. As shown in Fig. 1, materials selection is the first step towards making a biobased foam. Examples of common biobased materials are listed in Fig. 1 along with the key product properties that are typical of those materials. Materials selection then determines possible processing methods. Some processing methods, such as extrusion with a PBA, are relatively universal and can be applied to many different materials. Other methods may be completely exclusive to specific materials, such as the free-rise foaming of partially biobased polyurethanes. In general, each foaming method follows a few fundamental steps: (1) mixing of bulk materials and additives, (2) dispersion of a blowing agent within the bulk mixture, (3) phase separation of blowing agent from bulk to form voids. Beyond these fundamental steps however, the exact mechanisms of each foaming method vary. For example, in the extrusion method, the phase separation of the blowing agent from the bulk occurs *via* a drop in pressure, allowing the blowing agent to expand into a gas phase. Contrastingly, in the freeze-drying method, phase separation occurs when ice crystals are formed and the bulk material is no longer in solution.

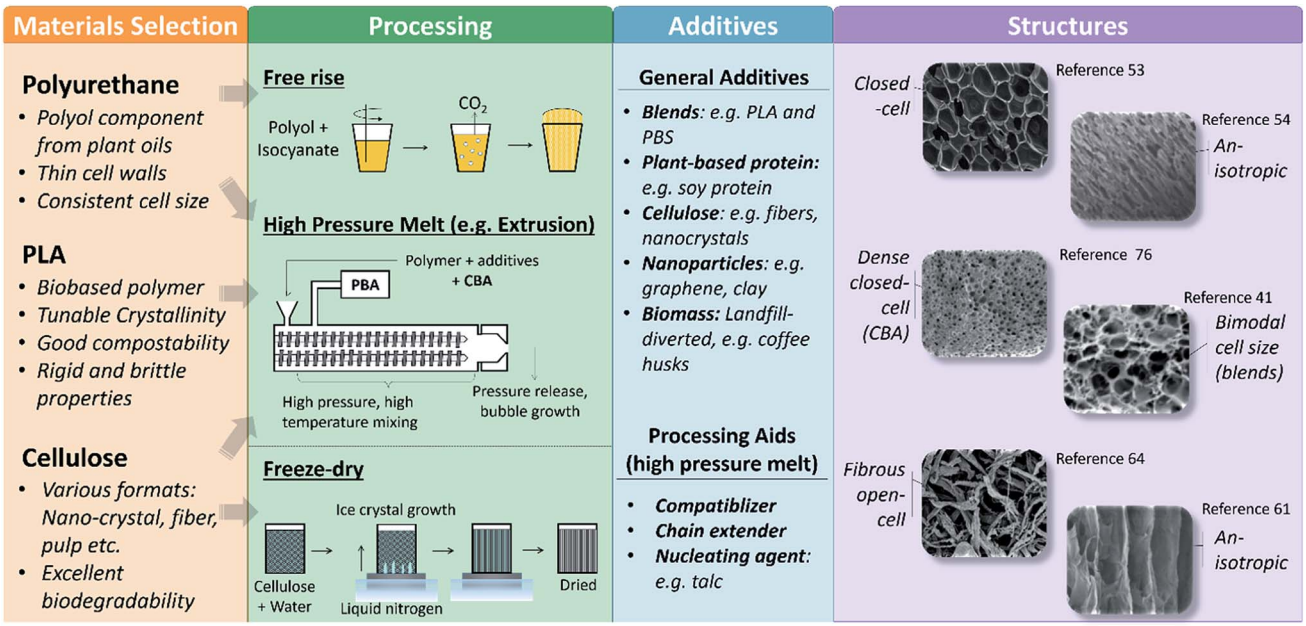

Fig. 1 Schematic plot summarizing biobased materials, their corresponding foaming methods, common additives, and possible foam structures. For simplicity, this review focuses on cellulose, polyurethane, and poly(lactic acid) (PLA) though other materials have also been explored. Portions of this figure have been adapted with permission from ref. 41, 53, 53, 61, 64 and 76.

The materials, processing, and additives collectively determine the foam structure and properties. Though some of the resulting foam structures are similar to foams made with traditional materials and foaming methods (*e.g.* XPS), there is a much wider variety in possible structures of biobased foams. As seen in Fig. 1, processing methods determined by the materials selection have influence on structure density, anisotropy, and closed-cell fraction. Typically, the factors which can alter foam structure include temperature, mixing parameters, pressure, time, blowing agents selection and additives. For example, extrusion can provide extensive control over the final structure through adjustments in temperature profile, screw rotation speed, screw element selection, *etc.*[31] The temperature of the polymer melt as it leaves the die is a determining factor in how much the foam is able to expand and how stable the foam structure is upon cooling. A very low temperature at the die could cause the outer skin of the foam to rapidly become rigid, preventing expansion. Contrastingly, a very hot temperature prevents the foam from becoming rigid quickly enough, resulting in collapse as it cools. Every processing method can produce multiple foam structure characteristics by adjusting method parameters.[15,23,36,41] In addition, additives influence the structure of foams in a variety of ways highly dependent on how the additive interacts with the bulk material and blowing agent. For instance, an additive which acts as a nucleating agent will typically reduce average cell size of the foam.[27] Alternatively, if an additive acts as a filler material (*e.g.* biomass) it may increase the foam density or disrupt the formation of cell walls, thus reducing the closed-cell fraction.[21]

The next sections will explore specific materials in depth and provide examples of biobased foam structures. Processing methods and additives will be discussed within the context of corresponding biobased materials rather than separately. This review will focus on some of the most popular biobased materials for producing foams, biobased polyurethanes, cellulose, and poly(lactic acid) (PLA).

2.1 Polyurethanes synthesized with biobased polyols

Traditional polyurethanes are made with petroleum-based components: polyols and isocyanates. Biobased polyurethanes are mostly synthesized using biobased polyols. Polyurethane foams are most commonly made using an exothermic "self-rising" method in which an isocyanate reacts with a water molecule and generates carbon dioxide gas.[49] Thus, water is referred to as a chemical blowing agent in this context. The nature of this foaming method tends to yield very low thermal conductivity foams with closed-cell structures and low density. Additionally, polyurethane (PU) foams have strong hydrogen bonding which results in superior mechanical properties relative to other traditional and biobased foams. Because these properties are so desirable, a vast amount of research has been dedicated to finding biobased replacements for the traditionally petroleum-based polyols.[16–22,50–56] The alternative polyols are commonly developed from different plant oils, of which the typical structure does not contain the functional groups (epoxy, amine, thiol, hydroxyl) necessary to react with the isocyanate. Most plant oils consist of a glycerol backbone and an oleic, a linoleic, and a linolenic acid chain.[50,51] In order to generate hydroxyl groups, these oils must first undergo an epoxidation reaction followed by opening up the epoxide ring. While shown to be successful in many cases, this modification will not always have the same results for every type of plant oil.[50,51] Castor oil is

an exception to this rule as it already contains the necessary functional groups to be reacted with isocyanates without modification. Compounded with the fact that each plant oil has different chemical structures to begin with, the type of oil used has a significant impact on the reaction with the isocyanate and the overall foam structure.

Most of these partially biobased PU foams share similar structure properties of closed cells and very high void fractions (*i.e.* percentage of void space within the foam). An example of this kind of structure can be seen in Fig. 2(a). The question of compostability must be addressed for these foams. Fig. 2(b) shows the results of a three-month composting experiment.[53] Some degradation clearly occurred. Although, given that the standard timescale for complete degradation of a compostable material is six months maximum,[57] it is not entirely plausible that these foams could be diverted from a landfill. Partially biobased PU foams already tend to display excellent low thermal conductivity properties. The next step in improving the sustainability of PU foams is by increasing biodegradability.

Partially biobased PU foams tend to be consistent with regard to having homogeneous, closed-cell structures. Some studies have shown, however, that adjusting foaming parameters can result in an increase or decrease of cell anisotropy. Fig. 2(c) shows an example of an array of anisotropic foams with cells elongated in the longitudinal (axial) direction. Under one condition, the cells actually became open pores. These foams were generated by adjusting the biobased polyol content along with the ratio of PBA (CO_2) to CBA (water) used.[54] The fact that an anisotropic foam structure can be formed both with this method for PU and with freeze dried cellulose (see Section 2.2)

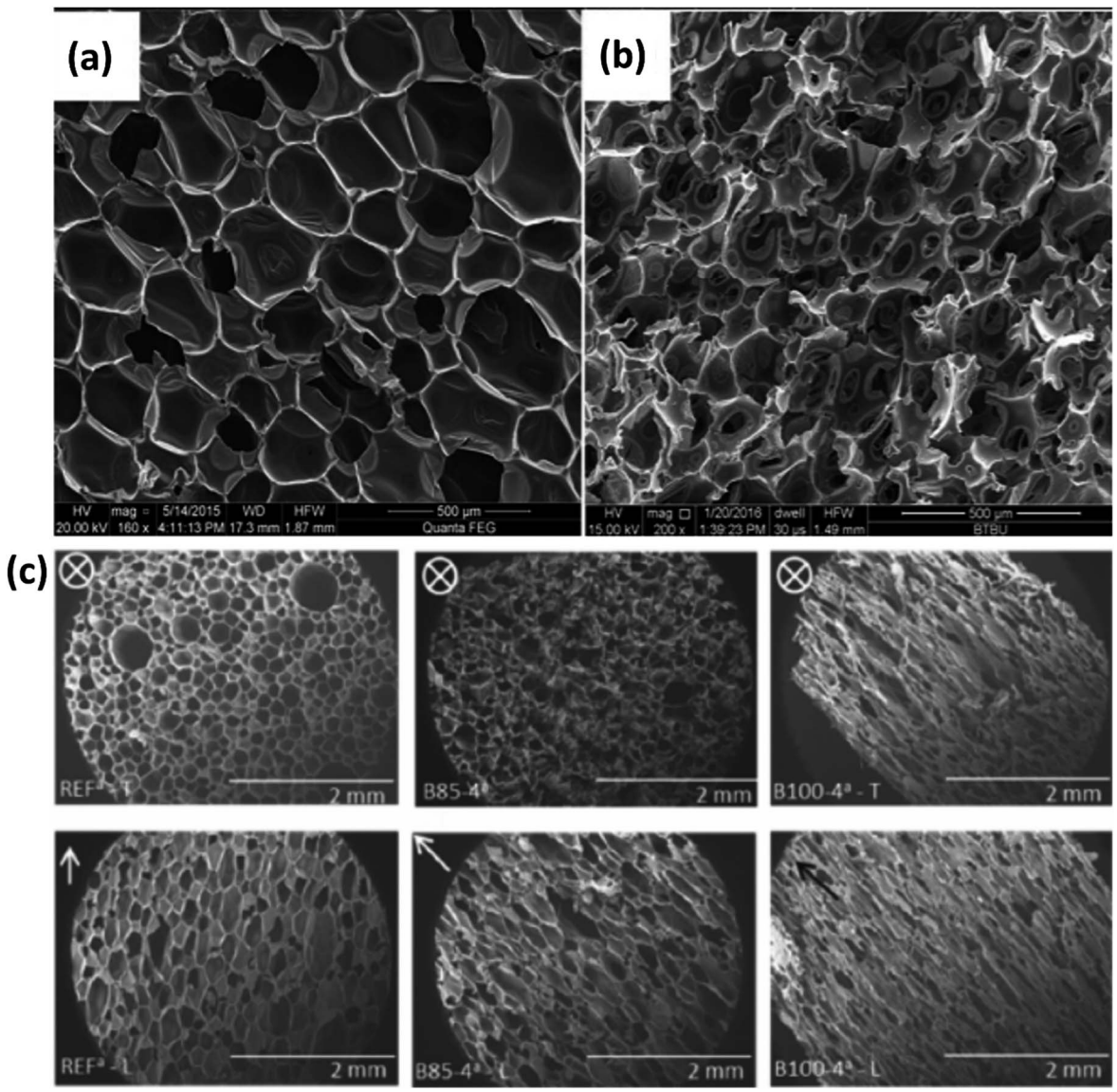

Fig. 2 Examples of partially biobased PU foam structures. (a and b) SEM micrographs of PU and soy protein composite foams (a) before and (b) after composting for 3 months reproduced from ref. 53 with permission from the authors, copyright 2018. (c) SEM micrographs of PU foam samples reproduced from ref. 54 with permission from Wiley, copyright 2018. Transverse (top) and longitudinal (bottom); biobased polyol percent from left to right: 0, 85, 100.[53,54]

exemplifies how much of an impact processing conditions have on the outcome of producing foams.

Though partially biobased PUs synthesized with plant oil polyols are the most common and most thoroughly developed form of biobased PUs, other chemistry approaches have been researched. In recent years, a significant amount of research has gone into developing PUs that do not require the use of isocyanates, which are petroleum-based and associated with toxic gases from synthesis.[58] One of the most common methods for generating non-isocyanate PU (NIPU) is through reacting cyclic carbonates and polyamines.[58] Both of these components can be synthesized from biobased sources through a variety of mechanisms. NIPUs, however, still require further research to make them competitive with traditional PUs from a processing standpoint as they typically suffer from low polymerization rate and unwanted side products.[58] Researchers have explored simpler methods to synthesize NIPUs, such as reacting sugars or lignin with a dimethyl carbonate component, forgoing the complex step of cyclization.[59,60] This secondary approach also has drawbacks such as the high temperatures required for foaming. More research is needed before NIPUs can become as scalable as biobased polyol PUs.

2.2 Cellulose

Cellulose is one of the most important biobased materials as it has abundant and diverse renewable sources. In addition, nano-

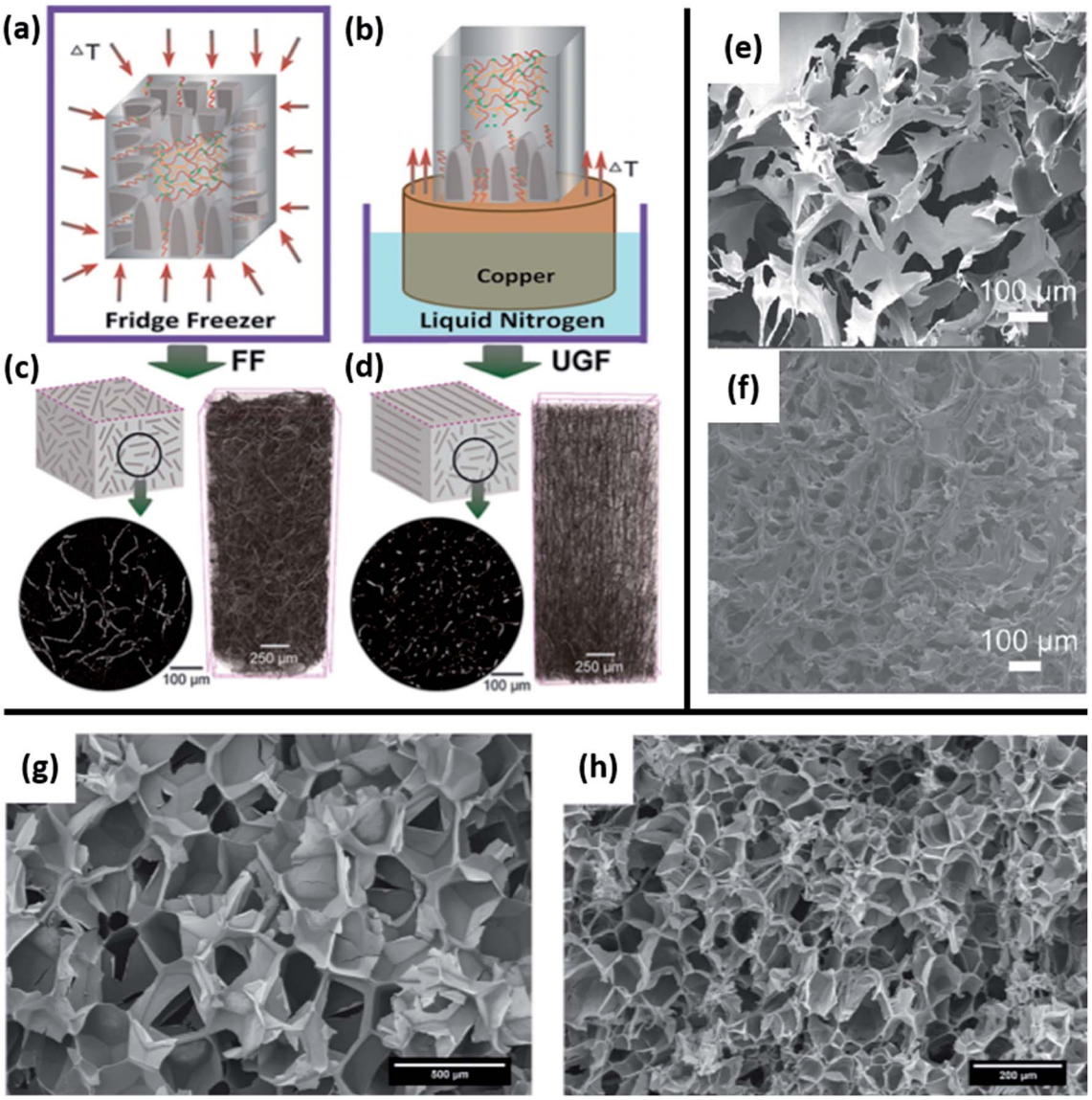

Fig. 3 Examples of cellulose foaming methods and structures. (a–d) Freeze drying conditions and structures for cellulose foam reproduced from ref. 61 with permission from American Chemical Society, copyright 2019. (a and b) Schematics of homogeneous freezer freezing (FF), unidirectional gradient freezing (UGF); (c and d) micro-CT scans of the foam structure for each freezing condition. (e and f) SEM micrographs of open-cell, non-ordered foams generated with homogeneous freeze drying conditions reproduced from ref. 14 with permission from Elsevier, copyright 2019. (e) Pure CNC foam; (f) CNC blend with 10% PVA and 25 wt% BTCA. (g and h) SEM images of extruded with isobutene used as PBA reproduced from ref. 65 with permission from Wiley, copyright 2019. (g) No cellulose added; (h) 20% cellulose fiber blend.[14,61,65]

cellulose fiber (NCF) and crystalline nano-cellulose (CNC) are of high interest as a sustainable material for use in composites for various applications. These composites can be categorized either as neat cellulose with added plasticizers or other processing aids, or cellulose as an additive in a polymer blend matrix.[35] The same categories are true for cellulose-based foams and both present their own opportunities and challenges for foaming. On its own, a cellulose-based material typically is not foamed using the traditional methods used to make EPS and XPS. For these cases, the most common method employed is freeze drying.[13–15,61–63] Mixing neat cellulose with water and other additives (*e.g.* surfactant, nanoparticles) and then freezing causes ice crystals to nucleate and grow surrounded by the cellulose matrix. After drying is complete, only the cellulose matrix remains with void space where ice had formed. A consequence of this method is that the direction of ice formation has a substantial impact on the foam structure. As shown in Fig. 3(a), the foam cell structure is essentially homogenous when an even temperature gradient is used (*e.g.* placing inside a freezer). However, there are downsides to this method of freezing as it can lead to cell collapse[61] and is generally not scalable or easily reproducible. It is also possible in homogeneous freezing conditions to form an open-cell, more disordered structure as opposed to a closed-cell structure as would typically be observed in EPS. If the temperature gradient is unidirectional as in Fig. 3(b), the cells become elongated in the axial direction. This kind of anisotropic structure will cause the thermal conductivity to differ depending on direction of measurement, with one study even reporting an order of magnitude difference between the radial and axial directions, radial having the lower value.[15] Other methods, less commonly used than freeze drying, for making neat cellulose foams have also been proposed. One alternative was presented by He *et al.* and involved vigorously mixing a solution containing cellulose pulp and a surfactant and then drying the solution without freezing or heating.[64] Similar to the structure shown in Fig. 3(e and f), the resulting foam had an open and fibrous structure.

When used as an additive or a component of a blend, cellulose often influences the structure of the resulting foam by altering melt flow. For example, one study which blended cellulose pulp with poly(lactic acid) (PLA) with a PBA extrusion foaming method reported that increasing the cellulose content in the blend resulted in reduced melt viscosity and smaller cell size displayed in Fig. 3(g and h).[65] The theory behind this phenomenon was that the cellulose acted as a nucleating agent by introducing interfaces where it is more energetically favorable for a bubble to form.[66,67] Additionally, the cellulose provided a kinetic barrier to PLA strand reconfiguration during bubble growth, thus restricting the expansion of each individual cell. The crystallinity of nano-cellulose additives can also

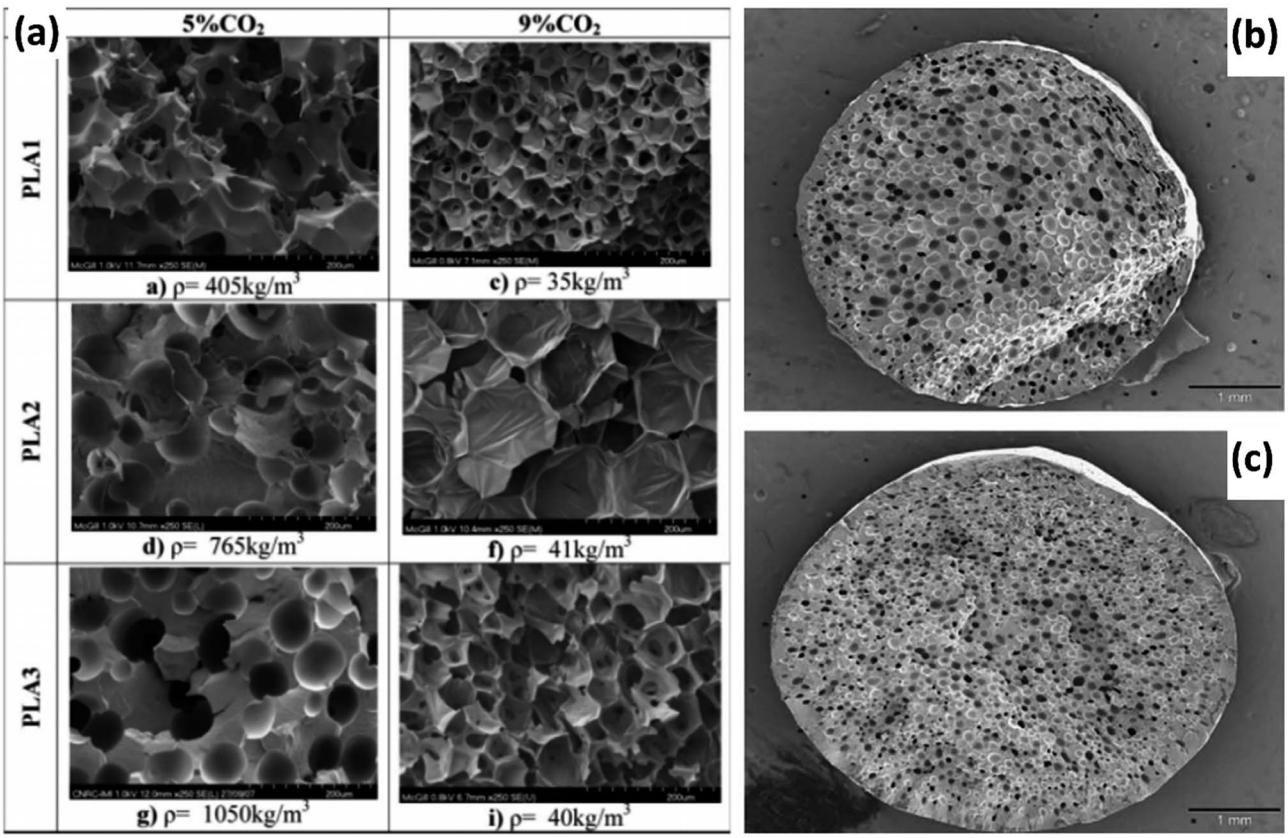

Fig. 4 Examples of PLA foam structures. (a) Impact of D-LA and PBA content on PLA foam structure and crystallinity: SEM micrographs corresponding to PLA1 (2% D-LA), PLA2 (4% D-LA), and PLA3 (10% D-LA) reproduced from ref. 40 with permission from Wiley, copyright 2009. (b and c) PLA foamed with endothermic CBA in extruder set at different screw speeds: (b) 20 rpm; (c) 120 rpm reproduced from ref. 76 with permission from Elsevier, copyright 2009.[40,76]

have an impact on the outcome. According to Stanzione *et al.*, amorphous and crystalline cellulose nanoparticles blended in a polyurethane foam both caused a reduction in cell size and a reduction in thermal conductivity.[68] The blends with amorphous particles, however, contained more fully closed cells (*i.e.* cell walls in tact) and had improved mechanical ductility compared to the blends with crystalline particles. This difference was attributed to the fact that the amorphous cellulose was more evenly dispersed and was more reactive with the isocyanate.

In summary, cellulose-based foams are made with a variety of methods. Freeze drying is most commonly used when cellulose is the primary component as opposed to a blend or an additive. Freeze drying has the potential to create interesting anisotropic structures which have been shown to very effectively reduce thermal conductivity in the radial direction. This method comes at the cost of scalability and reproducibility. As a result, cellulose is ultimately more often used as an additive in other foaming methods.

2.3 Poly(lactic acid)

PLA is a thermoplastic polyester derived from a variety of plant sources including corn, cassava, beets, and sugarcane. Various grades of PLA targeted at specific applications have been developed and are commercially available. Lactic acid monomers have two molecular configurations, L and D, in which the orientation of the methyl group is opposite (*i.e.* stereoisomers). The stereochemistry of PLA allows control over the polymer crystallinity. In a majority L-LA strand, increasing the D-LA content will result in the polymer becoming more amorphous.[69,70] As a result of its properties, which are often compared to polystyrene, and commercial availability, PLA has been a major material of interest for a multitude of applications including foams.[70] However, unlike polystyrene, PLA faces some major obstacles with regard to processing, namely degradation from water exposure and a lower glass transition temperature (approximately 60 °C). These issues can be avoided by ensuring material is properly dried and tuning the polymer architecture to optimize the crystallinity for stabilizing the foam structure.[69,70] Additionally, foam grade PLA is typically modified with a chain extender to improve its processing range and properties.[71,72]

Given the processing capability of PLA as a thermoplastic polymer, more traditional foaming methods, such as extrusion, injection molding, and autoclaving (*i.e.* enclosed in a high pressure, temperature controlled vessel) are employed.[23,25,73,74] PLA foams have been made with a variety of blowing agents. For PBAs, supercritical CO_2 ($scCO_2$) is usually preferred to N_2 due to the higher solubility of CO_2 as well as its known plasticizing effect on PLA.[40,69] Fig. 4(a) depicts the results of a study which

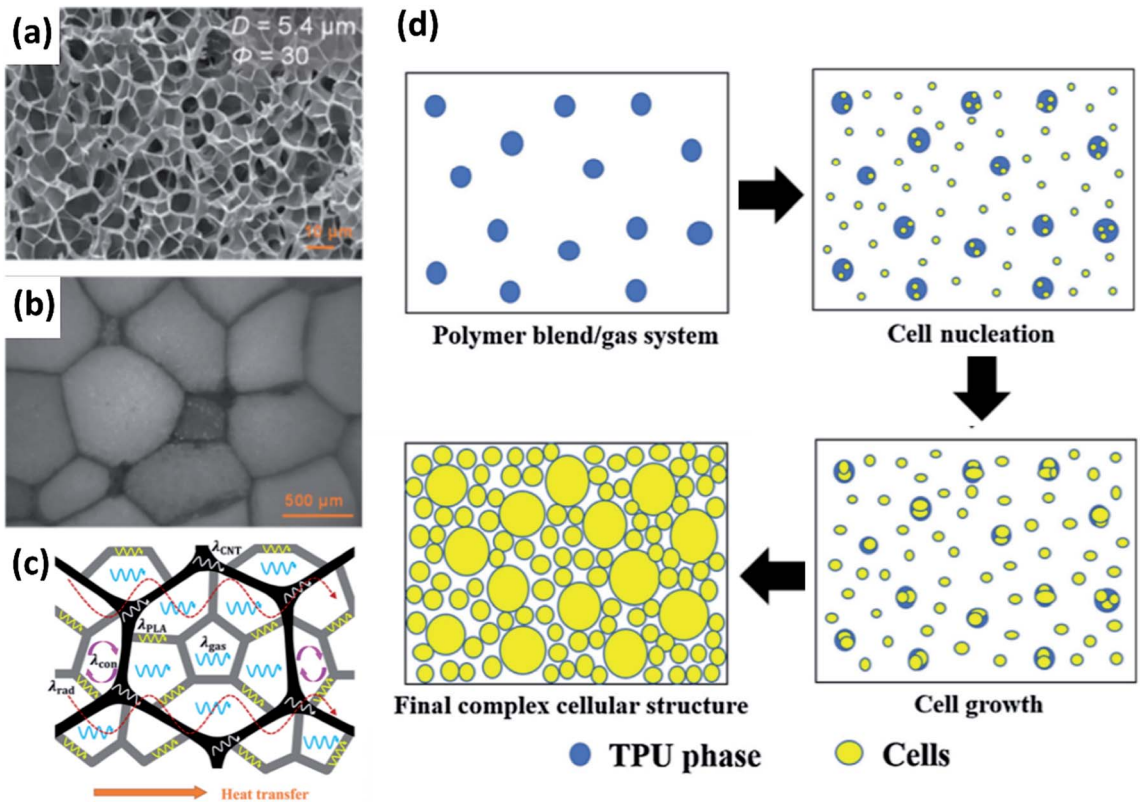

Fig. 5 Examples of PLA foam structures. (a–c) Foamed PLA beads wrapped in a carbon nanotube network reproduced from ref. 24 with permission from American Chemical Society, copyright 2017. (a) SEM micrograph of expanded PLA; (b) sintered expanded PLA beads with CNT network; (c) heat transfer diagram. (d) Schematic of proposed formation process of bimodal cell structure dependent on difference in nitrogen diffusion through the two polymer phases reproduced from ref. 41 with permission from Elsevier, copyright 2019. White areas denote PLA, blue areas denote thermoplastic PU, and yellow denotes a cell.[24,41]

explored the impact of D-LA content and amount of $scCO_2$ PBA.[73] The PLA with 2% D-LA content had the highest crystallinity that increased with the $scCO_2$ content, PLA with 4% D-LA had lower crystallinity, and PLA with 10% D-LA was completely amorphous regardless of $scCO_2$ content. Taking note of the density values measured for each sample along with physical structure, it is clear that designing the polymer to be partially crystalline allows for more expansion even at low PBA doses. More recent research has further explored the role of crystalline spherulites in bubble nucleation.[75]

CBAs have also been explored for use with PLA.[76,77] As is typical for CBAs in traditional foam practices, the resulting foams are denser than those made with PBAs. The structure of these dense foams can still be altered through other processing parameters, as shown in Fig. 4(b) and (c), although foam expansion is limited by the nature of CBAs.[76] However, CBAs can offer advantages as nucleating agents, to increase cell density and impede excessive bubble growth, maintaining a narrower distribution of cell size.[66,67] Other additives have been explored with the same goal of promoting nucleation and controlling cell structure. Some nanoparticle additives (*e.g.* nanoclay) have been found to contribute to other foam properties as well, such as mechanical strength.[52] Carbon nanotubes (CNTs) have also been used to generate an electrically conducting network within a PLA foam.[24,78] Wang *et al.* wrapped expanded PLA beads in a carbon nanotube network and then displayed how their own thermal conductivity model would need to be adapted to account for the network component shown in Fig. 5(a–c). Their model will be discussed later in this review (see Fig. 7).

PLA has also been the primary material of choice to explore unique biobased and partially biobased polymer blends. Blending polymers during foaming can lead to unique structures and properties. As was alluded to previously in this review, cellulose and PLA were extrusion foamed together while comparing isobutene and $scCO_2$ as PBAs.[65] The resulting foams (refer back to Fig. 3(h)) showed a clear trend of reducing cell size with increasing cellulose content regardless of the blowing agent. Cellulose, in this case, restricts the motion of the PLA chains during bubble growth. Another interesting blend, involving PLA and (non-biobased) thermoplastic PU, was studied by Qu *et al.* to determine the impact of using nitrogen as a PBA with two polymers with different N_2 solubility and diffusion coefficients.[41] The result was a bimodal distribution of cell sizes. The proposed mechanism behind this foam structure is summarized in Fig. 5(d). Thermal conductivity measurements revealed that this bimodal cell structure performed better as a thermal insulator than the even cell distribution foam used as a ref. 41 In summary, PLA foams, more so than other biobased foams, have a wide array of potential foaming methods and variables in processing that can be adjusted to create different structures.

2.4 Others

Other biobased materials have been explored for creating foams, including starch, plant-derived proteins and polybutylene succinate (PBS). Starch offers a great deal of flexibility in terms of possible foaming methods.[36] Extruded starch foams produce structures which are likely to have the greatest potential for thermal insulation applications.[36,79,80] Other methods, such as baking, freeze drying, and microwave heating have been demonstrated as well.[36,81] Most of the research regarding starch foams have focused on other applications than insulation such as foam trays to replace single-use disposable food packaging and foams with antimicrobial properties.[81,82] Much of the research has also focused on starch composite foams, incorporating other additives or blends. Engel *et al.* used grape stalks, generally considered a waste product, in their foams as a filler.[83] Similarly, Rojas *et al.* developed insulating foam using fibrous starch material from agriculture waste as the primary component.[84]

Plant-based protein plastics have limited processing capability, so require the use of plasticizers or blending with other polymers such as PU and PLA.[37,85–88] A great deal of work has gone into identifying effective biobased plasticizers. Foaming of these materials can be accomplished through methods such as injection molding.[37] It is important to note that plant-based proteins, while not as frequently used as the primary material in foams, are very often employed as additives to cross-link or otherwise adjust material properties.[53,89]

PBS foams are often made using similar methods to PLA foams. Injection molding and autoclave methods with $scCO_2$ as the blowing agent have produced a number of PBS foams with closed-cell structures.[90–92] Chemical blowing agents are also popular.[93–95] The focus of PBS foams research so far has been mainly on mechanical properties and the impact of processing aids such as plasticizers and cross-linking agents.[95–97] Beyond mechanical properties, one study incorporated carbon black nanoparticles into a PBS foam to increase electrical conductivity[90] and another reported achieving thermal conductivity as low as 0.022 W m^{-1} K^{-1} in a PBS foam by tuning endothermic and exothermic CBA components.[94]

There are more biobased materials and blends beyond what is discussed here.[98–101] It is important to emphasize that the research done with these materials shows as great deal of progress in the field. For the sake of simplicity, the remainder of the discussion on biobased foams in this review will focus on cellulose, PU, and PLA as the primary materials.

3. Heat transfer modelling

Thermal conductivity (*i.e.*, low thermal conductivity) is the most important parameter for temperature stabilizing packaging. The theoretical calculation of thermal conductivity is given in eqn (1), where thermal conductivity (k) has SI units of W m^{-1} K^{-1}, q is the heat flux, t is time, L is distance of heat transfer (*i.e.* material thickness), A is the area over which heat is transferred, and ΔT is the temperature difference.[102] Note that many publications use the symbol, λ, to denote thermal conductivity rather than k. It is important to understand the possible mechanisms for heat transfer and how to account for the foam structure when defining those mechanisms mathematically.

$$k = \left(\frac{q}{t}\right)\frac{L}{A\Delta T} \quad (1)$$

In general, there are three possible modes of heat transfer: conduction, convection, and radiation. For foam structures, convection is not typically a possible heat transfer mode, particularly for closed cell structures since air flow is restricted. While definite limits for which convection is negligible are debated, conservative estimates suggest that cells less than 3 mm in diameter or a Rayleigh number (relating to fluid flow turbulence) below 50 will meet the requirement.[103] Conduction in foams can occur through the solid material (foam structure) or gas conduction within the pores. Crucially, it must be recognized that for standard gas conduction conditions, the cell size must be greater than the mean free path distance of gas molecules (approximately 70 nm for air at room temperature).[104] When cell sizes fall below this distance and gas molecules are more likely to collide with cell walls than with other gas molecules, gas conductivity is reduced. This mechanism is known as the Knudsen effect.[104,105] Heat transfer *via* radiation is also possible in foams and, while conduction is usually the dominant mode, radiation can be a significant component as well.[43,44]

$$k_t = k_s + k_g + k_r \quad (2)$$

Each heat transfer mode will contribute towards the overall thermal conductivity of a foam as shown by eqn (2) where k_t is the total thermal conductivity, k_s is thermal conductivity from solid conduction, k_g is gas conduction, and k_r is thermal conductivity from radiation. Each of these individual terms can be defined using concepts from physics and mathematics, although not every model will define them in the same way. Thus, the differences between foam heat transfer models lie both in the assumptions made about foam structure as well as the theory behind heat transfer modes.

3.1 Model evolution: assumptions and validations

Thermal conductivity models have evolved significantly over time to incorporate both improved understanding of heat transfer mechanisms and more sophisticated modelling of foam structures. Early models took a one-dimensional approach to simplify the system while recent models have made use of stochastic generation algorithms to create virtual 3D structures. Each of these models, regardless of complexity, employ a base set of assumptions about heat transfer mechanisms and structure which range in validity. To understand how each model works and the context in which it could be reasonably used, these assumptions must be outlined.

One of the earliest models, commonly cited for its definition of radiative thermal conductivity, described microcellular polystyrene foams.[106] This model uses a simplistic design for foam structure: n layers of parallel polymer membranes of thickness L_s each separated by a gas layer of thickness L_g. This one-dimensional heat flow approach is not representative of real foam structures, but significantly simplifies calculations. The conduction contributions, solid and gas, are defined using Fourier's laws of heat conduction. This definition is now understood to be invalid for heat transfer through nanocellular structures,[107,108] but given the scope of this model only includes conventional foams with micro-scale cells, it is reasonable. The radiation contribution is calculated using refractive index and Bouguer's law to define the net fraction of radiant energy which passes through one solid membrane. The structure factor generated by the simple model geometry then is used to find the apparent radiative thermal conductivity for the full structure.

Some recent models have used similar approaches to define the structure of a foam.[42] Fig. 6(a) shows a one-dimensional heat flow structure. A major difference between this structure and the one-dimensional structure previously described is that the cell wall thickness and cell size are not fixed. Adjusting these parameters allows this model to describe the impact of porosity on thermal conductivity. This model improves its accuracy through a coupled approach to defining heat conduction and radiation which uses the steady state condition that the sum of the derivatives of each heat flux component must be zero. The radiative flux in this case was determined using a P_1-approximation.[46] The scope of this model encompasses both microcellular and nanocellular foams.[42] The findings of this model, shown in Fig. 6(b) and (c), suggest that generally, increasing porosity will decrease thermal conductivity. However, if wall size is held constant, the radiative contribution significantly increases at high porosity, as does total thermal conductivity.

The one-dimensional approach can provide valuable predictions for trends in thermal conductivity without the need to account for multiple paths of heat transfer. However, this

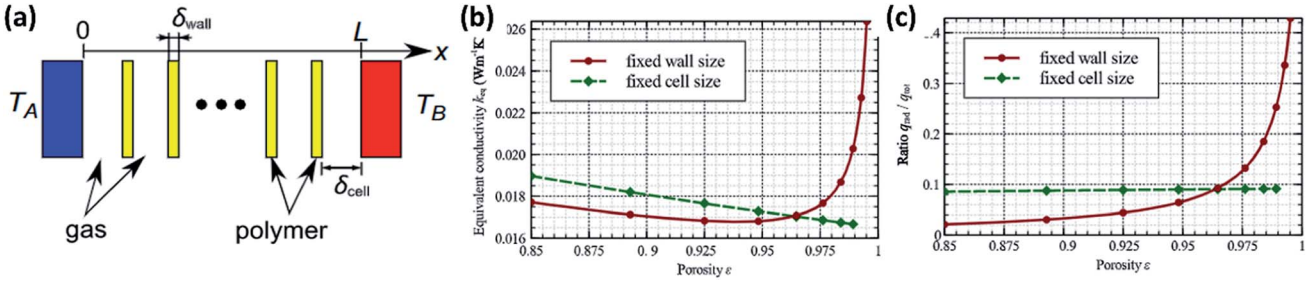

Fig. 6 One-dimensional heat transfer model diagram and trends. (a) Diagram of simplified foam structure. Trends in heat transfer relative to foam porosity while keeping either wall size or cell size fixed: (b) equivalent thermal conductivity; (c) ratio of radiative heat flux to total heat flux. Reproduced from ref. 42 with permission from Elsevier, copyright 2013.[42]

approach drastically simplifies the geometry. Several models have taken a more complex approach in the pursuit of more accurately describing real foam structures. Wang *et al.* proposed a 3-dimensional wall and strut model simplified to 2D to account for multiple possible paths for heat transfer in one direction.[47] A schematic of how this model was applied to determine the radiation component is shown in Fig. 7(a–e). This model applies the Knudsen equation for determining gas thermal conductivity over a range of possible cell sizes.[109] The model defines the Knudsen number, a dimensionless factor quantified as the ratio of the cell size to the mean free path of a gas molecule. Additionally, this model employed a characteristic size of the solid skeleton when calculating solid conductivity given that for nanocellular foams, boundary scattering of phonons at the cell walls becomes a significant factor.[110–112] Fig. 7(f) and (g) show the predictions for total thermal conductivity relative to void fraction and cell size. These results suggest that increasing void fraction will reduce thermal conductivity up to the point where the radiation component becomes more significant.[47] Additionally, very small (nanoscale) cell size has a dramatic effect, causing a thermal conductivity increase despite the Knudsen effect reducing the contribution from gas conduction.

The "wall and strut" method to constructing a foam skeleton harkens back to previous work by Smits, who developed a wall and strut model for polyurethane foams and explored polymer distribution in the foam structure.[113] Specifically of interest was what percentage of the material lies within the struts *versus* the walls at different cell sizes. The model predicted that the percentage of material in the walls increases for smaller cell sizes, leading to a trend in radiation opposite that of solid conduction. At small cell sizes, the cell walls are thicker films which can more readily block radiative heat transfer but allow more paths for phonon transport. Additionally, it is noted that if the foam density is reduced past a certain threshold point while maintaining cell size, the cell walls will no longer be stable resulting in an open cell structure.[113] This suggests that some characteristic cell wall thickness is likely specific to the foaming material. Since the cell walls act as a barrier to diffusion, the loss of cell wall stability thereby resulting in an open cell structure has major implications for foam thermal conductivity. Smits suggests that an open structure will have higher thermal conductivity than a closed structure with the same cell size and slightly higher density.

More recently, Bernardo *et al.* created a more structurally complex model to explore the impact of a bimodal cell size distribution.[48] Fig. 8(a) and (b) shows schematics of the model structure. Mathematically, this structure is described in two ways: series and parallel as shown in eqn (3) and (4) respectively. In the equations, λ_i and V_i are the thermal conductivity and volume fraction of the i-th phase. The reasoning to test both series and parallel approaches is to change the level of interaction between the two phases present (*i.e.* large cell phase and small cell phase).[114,115] It should be noted these models presented by Bernardo *et al.* only account for conduction, choosing to ignore radiation.[48] The results of the two models applied to a theoretical PMMA foam are displayed in Fig. 8(c). Increasing the fraction of nanocells decreases the thermal conductivity according to both series and parallel models. The impact of the width of the cell size distribution was also determined to be an important factor, with broader distributions resulting in higher thermal conductivity than narrower distributions even given the same average cell size.[48]

$$\lambda_t = \sum_{i=1,\,2} V_i \lambda_i \tag{3}$$

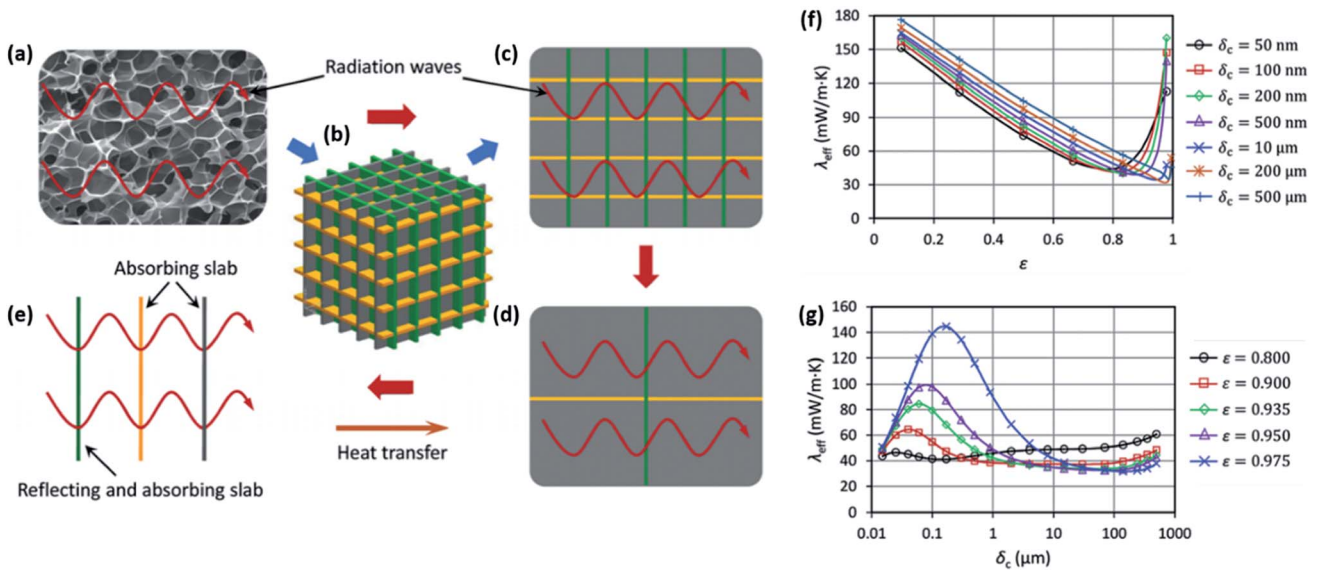

Fig. 7 Wall and strut heat transfer model. (a–e) Model schematic for radiative heat transfer. (a) Example of a real foam structure; (b) 3D model will cubic cells; (c) 2D representation; (d) 2D cubic unit cell containing three planes; (e) analysis model for a unit cell considering one reflecting slab and two absorbing slabs. Trends in total thermal conductivity relative to: (f) void fraction, ε, where each curve accounts for different cell size; (g) cell size where each curve accounts for different void fraction. Reproduced from ref. 47 from Royal Society of Chemistry, copyright 2017.[47]

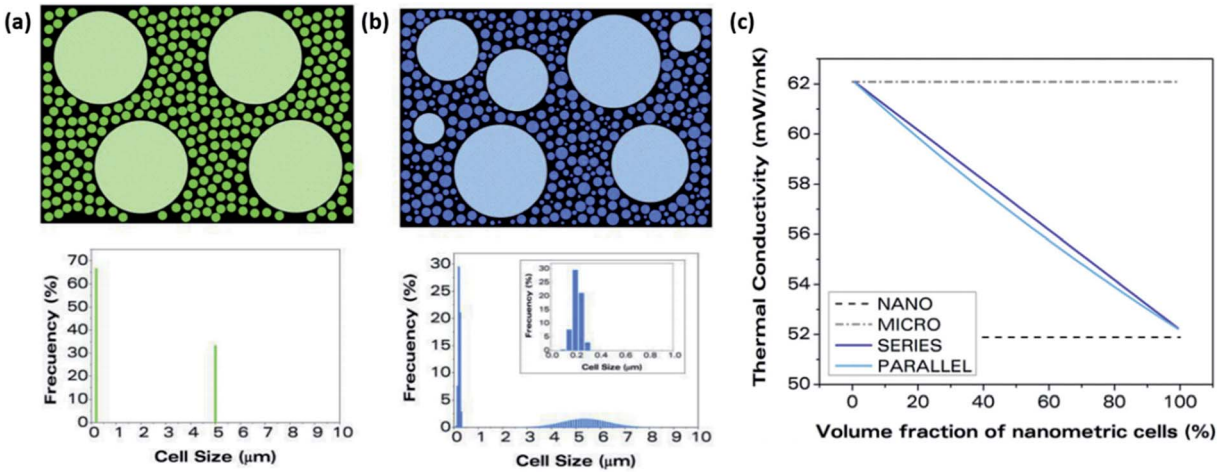

Fig. 8 Schematic of bimodal cell structure (a) accounting only for the two average cell sizes; (b) accounting for a full cell size distribution. (c) Series and parallel models for thermal conductivity of a bimodal structured PMMA foam with thermal conductivity determined relative to the volume fraction of the nanocell phase. Reproduced from ref. 48 with permission from Elsevier, copyright 2019.[48]

$$\frac{1}{\lambda_t} = \sum_{i=1,2} \frac{V_i}{\lambda_i} \quad (4)$$

All of the models discussed to this point have created simplified (to varying degrees) geometric approximations of real foam structures. In contrast, van de Walle *et al.* developed a model which employs micro-CT scanning and/or stochastic generation algorithms to get a more accurate representation of a true foam structure.[116,117] An overview of the simulation process is given in Fig. 9. The virtually produced structures were generated using stochastic algorithms exemplified in the previous literature.[118–121] The structures which this model is capable of analyzing are undoubtedly more accurate than those presented by the models previously discussed in this review. Of particular note, the usefulness of this model was demonstrated for granular foam structures (*e.g.* EPS). However, the more complex structures lead to more variables that must be accounted for within the thermal conductivity calculation. For this model, the thermal conductivity was calculated using the relatively simple approach of applying Fourier's heat conduction law, which has previously been shown to be invalid for nanocellular structures.[116]

3.2 Limitations of models

Due to the unusual physical structures of biobased foams, they are often not well represented in the previous models discussed. On the other hand, in recent years models have been considerably improved as the understanding of heat transfer mechanisms and structural factors has enhanced. Adapting current models to biobased foams will be an important future task in this field of study. The trends predicted by models can inform engineers and scientists developing new foam materials on the optimum structure to obtain the desired thermal conductivity.

It is still crucial to point out that all models have limitations. These limitations are perhaps best analyzed by compiling the assumptions upon which they are based. Table 1 gives a list of some major assumptions made in various models. The references used to make this assessment were chosen as they represent a variety of modelling approaches. Table 1 also provides a list of conclusions drawn from these models. By comparing the columns of Table 1, it is clear a few assumptions cannot accurately capture the key features of the foams. For example, the assumption that only average cell size needs to be considered as opposed to the full distribution is used in many models. However, Bernardo *et al.* concluded that the distribution has a major impact on thermal conductivity.[48] Other

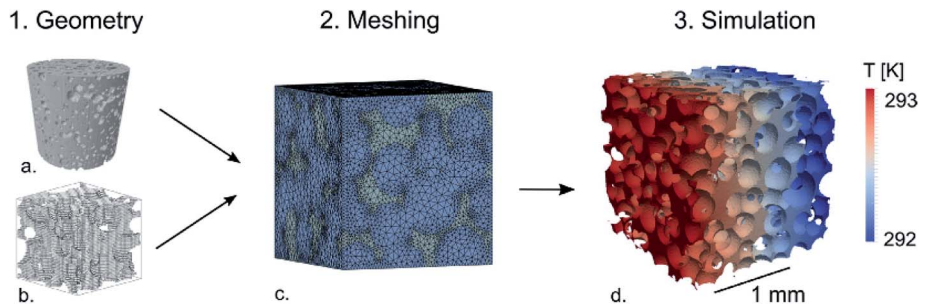

Fig. 9 Schematic of simulation process: (a) micro-CT image of real foam sample; (b) virtually generated image of foam structure; (c) finite element mesh applied to input; (d) simulation temperature profile. Reproduced from ref. 116 with permission from Elsevier, copyright 2018.[116]

Table 1 Assumptions regarding structure and heat transfer mechanisms and predictions made by a variety of thermal conductivity models[42,43,47,48,106,113,116,122]

Assumptions	References	Conclusions	References
Cells have a uniform size distribution	42, 43, 47, 106, 113 and 122	Conduction is the most significant mode of heat transfer	42, 43, 47, 48, 106 and 122
Considering only the average cell size is representative of the whole	42, 43, 47, 106, 113 and 122	Generally, reducing cell size reduces thermal conductivity	43, 47, 106, 113 and 122
Cells are generally spherical (isotropic)	42, 43, 47, 48, 106 and 122	Generally, increasing void fraction reduces thermal conductivity	42, 43, 47 and 116
Cells are closed	42, 43, 47, 48, 106, 113 and 122	Nanocellular foams display different trends than microcellular foams	47, 48 and 113
Convection is negligible	42, 43, 47, 48, 106, 113, 116 and 122	Impact radiation increases for high void fraction (low relative density) foams	42, 47 and 122
Radiation is ignored	48	Refractive index and absorption index have a significant impact on thermal conductivity	47 and 106
Reflectance and refraction index is constant for all cell sizes and void fractions	42, 43, 48, 106, 113, 116 and 122	Reflectance depends on cell size, void fraction, *etc.*	47
Consider only foam structure and primary material. No consideration for blends or additives	42, 43, 47, 48, 106, 113, 116 and 122	Width of cell size distribution is significant	48
Cell wall thickness remains essentially constant as cell size is changed	113	Changes in cell wall thickness and ratio of polymer present in cell walls to struts significantly impact thermal conductivity	113

problematic assumptions include neglecting the radiation component and taking the reflectance and refraction coefficients to be constant for all cell sizes and void fractions.

Furthermore, it is important to assess how well model assumptions apply to experimental systems. Table 2 compares model assumptions to observations in experimental biobased foams. It is clear that some foam structures, particularly open-cell and anisotropic structures, are not uncommon in biobased foams. Given that most current models do not account for these non-traditional structures, this presents a research gap. Micro-CT scanning of experimental foams to create structural information inputs for a model is a potential means fill this gap.[116] Additionally, all models assessed here have neglected to account for the possibility of polymer blends or solid

Table 2 Assumptions made in a variety of models corresponding to comparable observations in experimental biobased foams[13–24,26,27,41–43,47,48,54,62,64,73,106,113,116,122,123]

Assumption	References	Experiment observation	References
Cells have a uniform size distribution	42, 43, 47, 106, 113 and 122	Cells have a uniform size distribution	13, 14, 16, 17, 18, 20, 22, 23, 24, 62 and 123
		Cells have a bimodal size distribution	41 and 73
Cells are generally spherical (isotropic)	42, 43, 47, 48, 106 and 122	Cells are spherical (isotropic)	16, 17, 18, 23, 41 and 73
		Cells are oblong or cylindrical (anisotropic)	15, 20, 22, 54, and73
Cells are closed	42, 43, 47, 48, 106, 113 and 122	Cells are fully closed	17, 18, 22, 24, 41, 73 and 123
		Closed cell structure with significant portion of cells having ruptured walls	13, 16, 20, 21 and 54
		Cells are open	27, 62 and 64
Radiation is ignored	48	Radiation is a significant component	23 and 24
Consider only foam structure and primary material	42, 43, 47, 48, 106, 113, 116 and 122	Thermal conductivity changes with presence of additives or blends	13, 14, 17, 18, 20, 21, 24, 27, 41, 54, 64 and 123
		Foam structure changes with presence of additives or blends	15, 17, 18, 20, 21, 24, 27, 41, 54, 64 and 123

additives. Granted, it is not reasonable to consider every possible additive, but certainly it would be desirable to have a better understanding of how different polymer domains in a blend impact thermal conductivity depending on how those domains are arranged. An excellent example to demonstrate the importance of blends on the structure an experimental foam is given by Qu *et al.*[41]

4. Comparison of biobased foam properties

4.1 Raw data analysis

Due to the fact that so many variables impact the properties of biobased foams, it can be difficult to distinguish if any given material holds more promise for thermal insulation applications. Ideally, drawing a thorough and direct comparison between these experimental biobased foams would require datasets of thermal conductivity, apparent and relative density, average cell size, cell size distribution, closed cell fraction, and anisotropy ratio. These data would first help form an understanding of how these foams stack up purely on insulation performance (thermal conductivity) and then fully describe the foam structures to understand how any particular trends in structure are impacting performance.

In compiling performance data on cellulose, PU and PLA foams, it has become evident that reporting of the datum categories mentioned above in the literature is somewhat insubstantial. For example, many papers which list thermal insulation as a potential application for the experimental foam have not quantitatively described the foam structure or even measured thermal conductivity. This is in large part due to the fact that, in many cases, the focus of the research may not be thermal insulation properties. The result, however, is a gap between the amount of research assessing biobased foams and the amount of directly comparable data. Fig. 10 shows the references found by the authors to contain complete datasets for thermal conductivity arranged by primary foam material. Not only is the compiled dataset relatively small, it also contains huge fluctuations within materials and between materials. All three materials have at least one experimental foam that is on par or better than EPS/XPS. Additionally, PU foams seem to have more consistent thermal conductivity performance than cellulose and PLA. Besides these points, it is difficult to discern a clear trend from this figure alone. A few references display particularly large thermal conductivity ranges. Some of these can be explained by anisotropic foam structure, and others (shown shaded) are the result of adjusting blend components or additives.

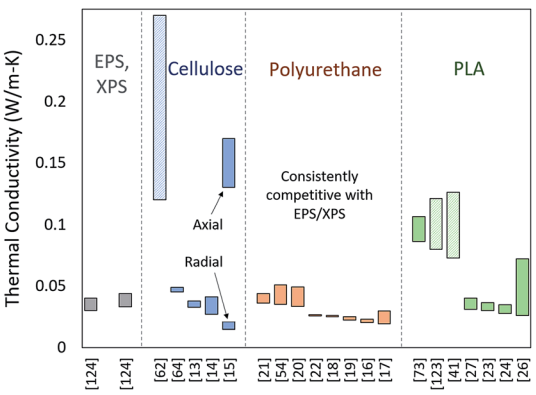

Fig. 10 Reported thermal conductivity ranges for experimental biobased foams arranged by material with EPS and XPS[124] and a general comparison. Bars that are shaded rather than solid indicate a large thermal conductivity range arising from additives or blends[15] has two ranges shown since the anisotropic foam samples were characterized in both the radial and axial directions.

Not all the papers reported thermal conductivity values together with quantitative structure data, which makes it difficult to compare the performance precisely. There are multiple potentially informative structural characteristics which are underreported. Of the biobased foams which report thermal conductivity, the most commonly reported structure characterizations are apparent density and average cell size shown in Fig. 11(a) and (b). It is immediately evident that apparent density is not very informative and does not follow any clear trend even among similar materials. The lack of trends is initially confusing given that several models previously discussed in this review specifically show the impact of void fraction (or equivalent terms), which is a term derived from apparent density. Similar to apparent density, the average cell size data does not reveal any useful information. Complete cell size distribution parameters are very rarely reported and having only average cell size makes it far more difficult to compare foams with non-traditional structures. Some have specified directionality of the cell size measurement if the foam was anisotropic, but fewer have provided an anisotropy ratio or measurements in other directions. The thermal conductivity value of anisotropic foams is also typically only measured in one direction, and at times, directionality is not specified. Notably, both the compiled density and cell size data do not follow clear trends. Very little insight could be gained from either of these plots.

The lack of comprehensive datasets posts a barrier in understanding the true performance of these experimental biobased foams. At this point, one option is to look for models that may allow us to better understand the relationship between foam structure and properties. Refining models will lead to better predictions for foams with non-traditional structure characteristics, and ultimately, fill in these data gaps. An alternative approach is to display the data that are already available and fit the gap through a simple mathematical dimensional analysis.

4.2 Dimensional analysis approach

To make better use of the data available, the most commonly reported structural characteristics, apparent density and average cell size, must be compiled and translated into a form which is possible to directly compare across studies. Apparent density is problematic since it is not directly comparable across studies; different materials and blends cause differences in

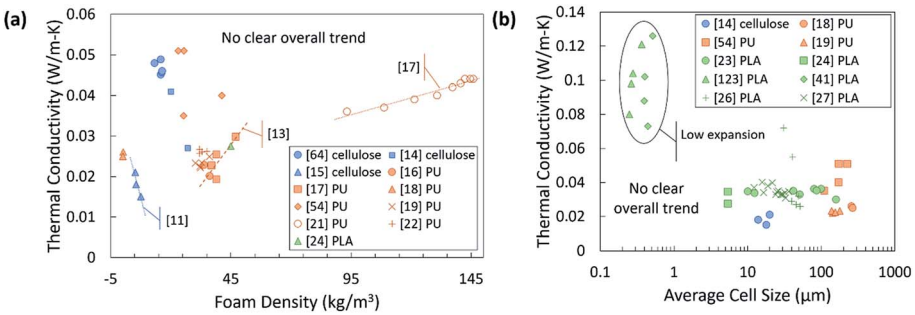

Fig. 11 Reported thermal conductivity data relative to (a) apparent density and (b) average cell size. Blue points are cellulose, orange points are PU, and green points are PLA. The points plotted from ref. 15 are specifically thermal conductivity measurements in the radial direction.[41] Foam samples were bimodal; the average size of the smaller cells is plotted here. A few trend lines are added for samples from the same reference.

density not related to foam structure. One way to make apparent density data more useful is by translating it into relative density, *i.e.* the density of the foam divided by the density of the bulk material prior to foaming. Relative density is valuable since it removes the specific material properties from the picture, making it easy to compare across datasets. Reporting of either expansion ratio (the inverse of relative density) or void fraction (one minus the relative density) is equivalent.

The only group of biobased foams for which all these data are available is closed-cell PLA foams, shown in Fig. 12. These data follow a clear trend, similar to other plots of compiled data in previous literature which include more traditional insulation materials such as EPS or polypropylene foams. It would indicate that thermal conductivity is low for high expansion ratio (*i.e.* low relative density) foams and increases rapidly in low expansion ratio ranges. The fact that these particular PLA foams follow this trend is unsurprising since the structures involved are on the whole quite similar to traditional foams. From a theoretical standpoint, the power law behavior is supported by the fact that solid conduction will be very high when foams are very dense. The introduction of any barriers (cells) to phonon transport should cause the solid conduction to rapidly decrease. Then, as the foam becomes mostly void space, the foam should asymptotically approach the thermal conductivity of air.

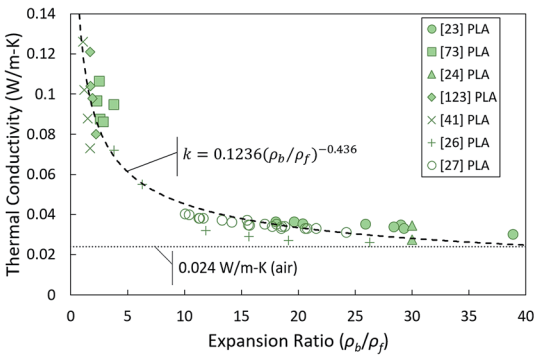

Fig. 12 Reported thermal conductivity data relative to expansion ratio (density of bulk non-foamed material divided by the density after foaming). A trend line fitting the data is shown with the corresponding equation.

Given the strong trend revealed here with relative density, it stands to reason that displaying foam structural and thermal data in relative, dimensionless terms is needed to obtain useful insight. In particular, a dimensionless approach to data analysis could be valuable for foams with complex, non-traditional structures for which it is difficult to accurately apply current models. Here, we propose a rudimentary dimensional analysis approach to help fill in the data gaps. The mathematical fit was constructed using the datasets previously analyzed in Section 4.1. It is important to note that this method does not rely on true physical understanding of the material structures. It is only based on mathematical correlation.

To make the available data on biobased foams easier to compare, all variables involved were first made to be dimensionless. Table 3 shows a summary of how all variables for this analysis were defined. Relative thermal conductivity, k_{rel}, was calculated by dividing measured foam thermal conductivity values by the assumed thermal conductivity of the bulk material. Values of bulk material thermal conductivity are given in Table 3. It should be noted that it is not necessarily accurate to assume that all the solid materials used to make these experimental foams had these thermal conductivities, but there are not substantial data provided to improve this assumption. Similarly, the relative density, ρ_{rel}, was calculated by dividing the reported apparent foam densities by the assumed density of the solid material (see Table 3). The calculation of relative density was not necessary in all cases since some studies reported expansion ratio, which is the inverse of relative density. Thus, the assumed solid material density values were only employed when expansion ratio data was not available. To transform reported average cell sizes into a dimensionless parameter, d_{rel}, the measured average cell size was divided by a theoretical maximum cell size, d_{max}. The calculation of d_{max} is done by assuming a one meter cube of material containing a single cell, large enough to achieve the void fraction of the foam. Consequently, d_{rel} essentially reflects the number of barriers to heat transfer in 1 meter of material. A smaller d_{rel} implies a larger number of barriers that must be passed to get from one end to the other.

All references from which data was pulled to calculate our mathematical fit have reported thermal conductivity, average

Table 3 Definitions of measured and dimensionless variables and numerical values of bulk material variables used in the dimensional analysis

Property	Measured variables	Dimensionless variables
Thermal Conductivity (k)	$k_f \equiv$ foam k $k_b \equiv$ bulk material k $k_{cellulose} = 0.23$ W m^{-1} K^{-1} (ref. 125) $k_{PU} = 0.19$ W m^{-1} K^{-1} (ref. 126) $k_{PLA} = 0.18$ W m^{-1} K^{-1} (ref. 127)	$k_{rel} = \frac{k_f}{k_b}$
Density (ρ)	$\rho_f \equiv$ foam apparent ρ $\rho_b \equiv$ bulk material ρ $\rho_{cellulose} = 1500$ kg m^{-3} (ref. 128) $\rho_{PU} = 1225$ kg m^{-3} (ref. 126) $\rho_{PLA} = 1240$ kg m^{-3} (ref. 129)	$\rho_{rel} = \frac{\rho_f}{\rho_b}$ Expansion ratio $\equiv \theta = 1/\rho_{rel}$ Void fraction $\equiv \gamma = 1 - \rho_{rel}$
Average cell size (d)	$d \equiv$ measured average cell size $d_{max} \equiv$ max cell size in 1 m^3 at given γ $d_{max} = (1\ \text{m}^3\gamma)^{\frac{1}{3}}$	$d_{rel} = \frac{d}{d_{max}}$

cell size, and either apparent foam density or expansion ratio. After converting all variables into dimensionless forms, a predicted k_{rel} was calculated from d_{rel} and ρ_{rel} using eqn (5) where x and y are the respective fit parameters. The solver function in Microsoft® Excel® was used to minimize the mean square error between predicted k_{rel} and the measured k_{rel} by adjusting x and y. Errors were given different weighting depending on the density data available. If expansion ratio was measured and reported directly, the point was given weighting of 1. If only apparent density was reported and relative density had to be calculated using material constants in Table 3, the point was given a weighting of 0.5. Fig. 13 displays the master curve of the measured *versus* predicted relative thermal conductivity and the final fit equation with optimized x and y. If the correlation were perfect, all points in the master curve would lie along the diagonal. There are some clusters of data which deviate from the trend, but in general, the equation fits reasonably well. Unsurprisingly, the optimized value for y is remarkably close to the exponent for the trend line observed in the reported expansion ratio data shown in Fig. 12. The same optimization process was done considering only d_{rel} or ρ_{rel} and with/without weighting errors. The results of each scenario are given in Table 4. Regardless of weighting, including both d_{rel} and ρ_{rel} minimizes the error of the prediction. It is notable, however, that ρ_{rel} on its own is a far better predictor of thermal conductivity than d_{rel} despite the fact that d_{rel} is affected by both cell size and density.

$$k_{rel} = {d_{rel}}^{x}{\rho_{rel}}^{y} \quad (5)$$

To assess the trends presented by our mathematical fit and begin to fill data gaps, cell size and relative density data for biobased foams that do not have reported thermal conductivity values have been compiled in Fig. 14(a). These data were selected as they encompass a wide range of relative density and cell size. The predicted k_{rel} values were then plotted with the reported cell size in Fig. 14(b). This data was overlaid with four theoretical curves produced from the optimized eqn (5). Each curve corresponds to a fixed ρ_{rel} value. The curves display how k_{rel} changes with cell size given that fixed value for ρ_{rel}. These curves suggest that at very low relative densities, changes in cell size have virtually no impact on foam thermal conductivity. However, at higher relative densities, a change cell size can be quite significant, particularly if transitioning from

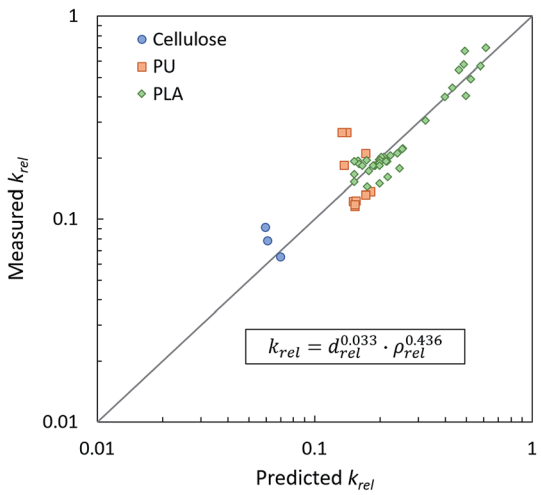

Fig. 13 Master curve of measured relative thermal conductivity *vs.* predicted relative thermal conductivity.

Table 4 Results of Excel® Solver optimization for different prediction equations with and without error weighting

Prediction equation		X	Y	Mean squared error
Weighted errors	$k_{rel} = {d_{rel}}^{x}{\rho_{rel}}^{y}$	0.03288	0.43578	0.03179
	$k_{rel} = {d_{rel}}^{x}$	0.12835	—	0.43044
	$k_{rel} = {\rho_{rel}}^{y}$	—	0.54263	0.06549
Unweighted errors	$k_{rel} = {d_{rel}}^{x}{\rho_{rel}}^{y}$	0.03472	0.42473	0.04787
	$k_{rel} = {d_{rel}}^{x}$	0.13658	—	0.52388
	$k_{rel} = {\rho_{rel}}^{y}$	—	0.52914	0.08776

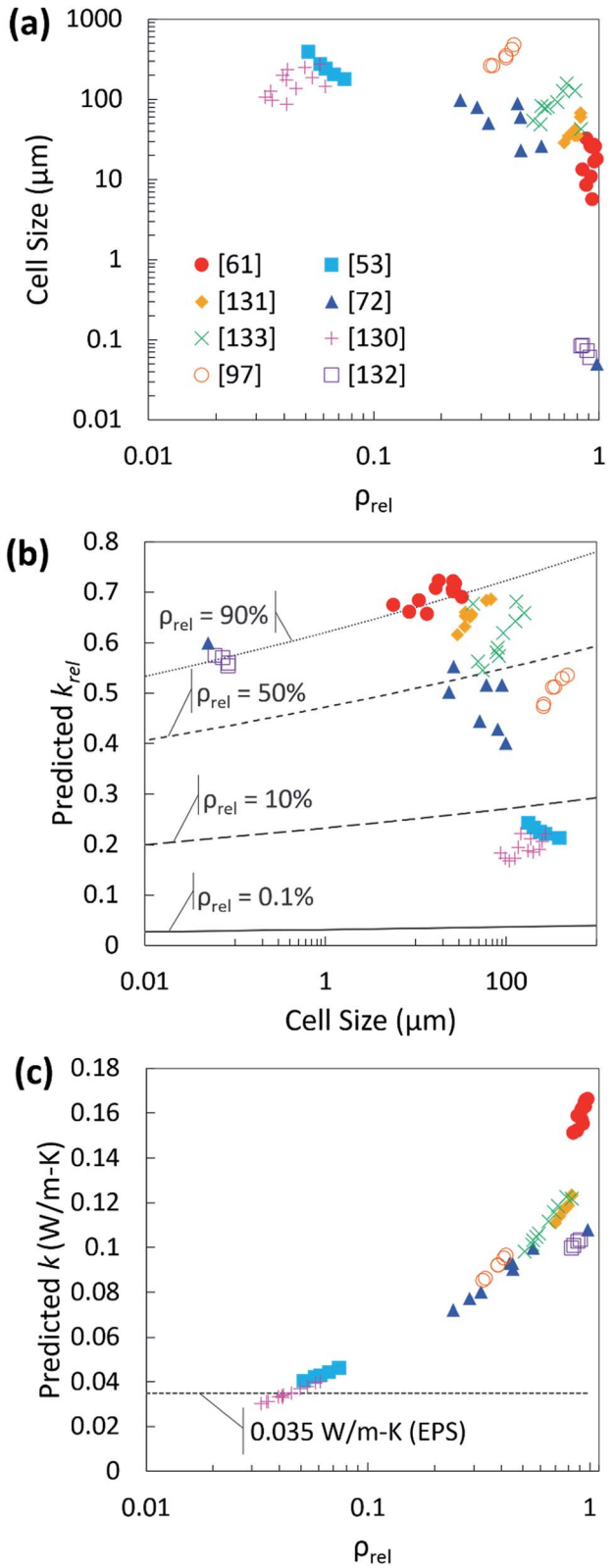

Fig. 14 (a) Compiled biobased foam relative density and cell size data;[53,61,72,97,130–133] (b) predicted k_{rel} plot for compiled data in terms of cell size overlaid with theoretical curves produced by the dimensional analysis fit equation showing impact of cell size for four different values of ρ_{rel}; (c) predicted k_{rel} converted to predicted effective thermal conductivity and plotted relative to ρ_{rel}.

a nanocellular foam to a microcellular foam or *vice versa*. It should also be noted that some regions of the theoretical curves are not necessarily possible in real foams; it is unlikely to achieve a foam with both very low density and very small cell size. Therefore, the most important observation from this analysis is that for thermally insulating foams, low relative density is the most influential factor with cell size being somewhat inconsequential. The predicted effective thermal conductivity of the compiled data was obtained by multiplying the predicted k_{rel} values by the appropriate material thermal conductivity constants in Table 3. As seen in Fig. 14(c), only two of the studies have predicted values which compare with the thermal conductivity of EPS: Li *et al.* created low density PLA foams using a high pressure vessel with CO_2 as a PBA[130] and Zhang *et al.* created a castor oil-based PU foam with soy protein as a crosslinking agent using the free-rise foaming method.[53]

The dimensional analysis shown here is by no means comprehensive and it has not been validated experimentally. It should also be noted that, given the limitations of the available data, our mathematical fit provides no insight to how specific heat transfer mechanisms impact the thermal conductivity nor does it identify how foams with specific, non-traditional structures behave. The purpose of generating this correlation was twofold. First, the dimensional analysis explores a different approach to predicting thermal conductivity. Second, it provides a preliminary method for filtering through data in biobased foams literature to predict which experimental foams are most promising for thermal insulation. The analysis is not without merit, as it identified a trend in cell size which is not initially apparent from the raw data. Specifically, it suggests that the impact of cell size cannot be viewed independently of relative density. It also demonstrates the potential value in creating a model which is adaptive. The exponential fit parameters in our analysis can be adjusted as more data are added in the future. This will enable us to predict the thermal conductivity, cell size, or relative density for foams where the structure has not been thoroughly characterized. Furthermore, when more data for other structural characteristics becomes available, it is straightforward to add new fitting parameters or combine with current ones in the analysis.

5. Concluding remarks

Great strides have been made in recent years in the development of biobased foams for many applications including thermal insulation. The wide variety of materials and processing methods result in a diverse range of foam structures. Several experimental foams have already demonstrated thermal conductivity that is competitive with the industry standard. It would be ideal to benchmark the performance of these foams quantitatively and determine if there is any preferable structure, material and/or additive for producing biobased insulating foams. However, the lack of comparable data makes such an assessment challenging.

The field of heat transfer modelling has also made impressive improvements, both in terms of more accurately reflecting true foam structures and calculating the contributions of

individual heat transfer modes. As a result, these models have enabled researchers to identify the structural features which are desirable for thermally insulating foams and adjust processing conditions to achieve those structures. Notable structure features including, closed *versus* open cells, cell anisotropy, cell wall thickness and cell size distribution, are all shown to relate directly to thermal conductivity and other foam properties. The importance of heat transfer models in helping to inform new research endeavors cannot be understated. There remains a gap however, between what information current models can provide and the foam structures which are possible experimentally, particularly for biobased foams. Therefore, it is important to engage an adaptive approach. This may not only help fill the data gap in characterization of biobased foams, but also deepen our understanding of foam structure–property relationships.

There remain ways in which the properties of biobased foams could be improved and there is a need to more thoroughly compare those properties. Some foams have achieved highly desirable properties but are only partially biobased. Some materials have extremely wide ranges of thermal conductivity depending on additives and processing conditions. Additionally, the foaming methods which can be employed are limited by the material being used. Finding ways to manipulate biobased materials to improve the ease of processing is crucial from a practicality standpoint and would broaden potential capabilities. The complexity in foaming process and unknown variables post challenges in biobased foam research. On the other hand, these challenges also represent opportunities. Current and future heat transfer models may serve as a means to help address the challenges specific to processing conditions and material properties. The results will enable further progress by providing insight to structure property relationships for biobased foam systems.

Conflicts of interest

There are no conflicts to declare.

Acknowledgements

The authors would like to thank the Polymer and Food Protection Consortium at Iowa State University for funding this work.

References

1 E. Olson, F. Liu, T. Bahns, S. Jiang, K. Vorst and G. Curtzwiler, *Sustainable Mater. Technol.*, 2020, **25**, e00193.
2 E. Olson, Y. Li, F.-Y. Lin, A. Miller, F. Liu, A. Tsyrenova, D. Palm, G. W. Curtzwiler, K. L. Vorst, E. Cochran and S. Jiang, *ACS Appl. Mater. Interfaces*, 2019, **11**, 24552–24559.
3 S. Chen, E. Olson, S. Jiang and X. Yong, *Nanoscale*, 2020, **12**, 14560–14572.
4 S. Jiang, A. Van Dyk, A. Maurice, J. Bohling, D. Fasano and S. Brownell, *Chem. Soc. Rev.*, 2017, **46**, 3792–3807.
5 D. Maga, M. Heibel and V. Aryan, *Sustainability*, 2019, **11**, 5324.
6 C.-A. Gabriel, N. A. Bortsie-Aryee, N. Apparicio-Farrell and E. Farrell, *J. Cleaner Prod.*, 2018, **182**, 1095–1106.
7 F. Razza, F. Degli Innocenti, A. Dobon, C. Aliaga, C. Sanchez and M. Hortal, *J. Cleaner Prod.*, 2015, **102**, 493–500.
8 C. Inagrao, A. Lo Guidice, J. Bacenetti, A. Mousavi Khaneghah, A. S. Sant'Ana, R. Rana and V. Siracusa, *Food Res. Int.*, 2015, **76**, 418–426.
9 A. Zabaniotou and E. Kassidi, *J. Cleaner Prod.*, 2003, **11**, 549–559.
10 C. Inagrao, A. Lo Guidice, J. Bacenetti, A. Mousavi Khaneghah, A. S. Sant'Ana, R. Rana and V. Siracusa, *Food Res. Int.*, 2015, **76**, 418–426.
11 G. Kale, T. Kijchavengkul, R. Auras, M. Rubino, S. E. Selke and S. P. Singh, *Macromol. Biosci.*, 2007, **7**, 255–277.
12 E. Chiellini and R. Solaro, *Adv. Mater.*, 1996, **8**, 305–313.
13 S. Ahmadzadeh, A. Nasirpour, J. Keramat, N. Hamdami and T. Behzad, *Colloids Surf., A*, 2015, **468**, 201–210.
14 P. Wang, N. Aliheidari, X. Zhang and A. Ameli, *Carbohydr. Polym.*, 2019, **218**, 103–111.
15 B. Wicklein, A. Kocjan, G. Salazar-Alvarez, F. Carosio, G. Camino, M. Antonietti and L. Bergström, *Nat. Nanotechnol.*, 2015, **10**, 277–283.
16 D. Ji, Z. Fang, W. He, K. Zhang, Z. Luo, T. Wang and K. Guo, *ACS Sustainable Chem. Eng.*, 2015, **3**, 1197–1204.
17 R. Yang, B. Wang, M. Li, X. Zhang and J. Li, *Ind. Crops Prod.*, 2019, **136**, 121–128.
18 J. Paciorek-Sadowska, M. Borowicz, B. Czuprynski and M. Isbrandt, *Polymers*, 2018, **10**, 1334.
19 P. Furtwengler, R. M. Boumbimba, A. Sarbu and L. Averous, *ACS Sustain. Chem. Eng.*, 2018, **6**, 6577–6589.
20 B. Li, M. Zhou, W. Huo, D. Cai, P. Qin, H. Cao and T. Tan, *Ind. Crops Prod.*, 2020, **143**, 111887.
21 N. Gama, L. C. Costa, V. Amaral, A. Ferreira and A. Barros-Timmons, *Compos. Sci. Technol.*, 2017, **138**, 24–31.
22 A. Arbenz, A. Franche, F. Cuttica and L. Averous, *Polym. Degrad. Stab.*, 2016, **132**, 62–68.
23 P. Gong, S. Zhai, R. Lee, C. Zhao, P. Buahom, G. Li and C. B. Park, *Ind. Eng. Chem. Res.*, 2018, **57**, 5464–5471.
24 G. Wang, L. Wang, L. H. Mark, V. Shaayegan, G. Wang, H. Li, G. Zhao and C. B. Park, *ACS Appl. Mater. Interfaces*, 2018, **10**, 1195–1203.
25 K. Parker, J.-P. Garancher, S. Shah and A. Fernyhough, *J. Cell. Plast.*, 2011, **47**, 233–243.
26 G. Wang, J. Zhao, G. Wang, H. Zhao, J. Lin, G. Zhao and C. B. Park, *Chem. Eng. J.*, 2020, **390**, 124520.
27 J. Wang, J. Chai, G. Wang, J. Zhao, D. Zhang, B. Li, H. Zhao and G. Zhao, *Int. J. Biol. Macromol.*, 2019, **138**, 144–155.
28 C. J. Cleveland, *Energy*, 2005, **30**, 769–782.
29 R. Kunic, *Energy Effic.*, 2017, **10**, 1511–1528.
30 S. Lee, R. Smith, S. Costeux, J. Alcott, M. Barger, D. Beaudoin, H. Clayton, S. Donati, J. Duffy, R. Fox, D. Frankowski, K. Giza, L. Hood, T. Hu, C. Kruse, T. Morgan, C. Shmidt, W. Stobby and C. Vo, presented in part at the, *SPE FOAMS*, Iselin, NJ, 2009.
31 T. Pontiff, in *Foam extrusion: principles and practice*, ed. S. T. Lee, Technomic Publishing Company, Lancaster, PA, 2000.

32 M. Chandra, C. Kohn, J. Pawlitz and G. Powell, *Real cost of styrofoam*, Saint Louis University, 2016.
33 EUMEPS, *EPS recycling international*, https://epsrecycling.org/global-recycling-access, 2020.
34 G. Wypych, *Handbook of foaming and blowing agents*, ChemTec Publishing, Toronto, CA, 1st edn, 2017.
35 R. J. Moon, A. Martini, J. Nairn, J. Simonsen and J. Youngblood, *Chem. Soc. Rev.*, 2011, **40**, 3941–3994.
36 N. Soykeabkaew, C. Thanomsilp and O. Suwantong, *Composites, Part A*, 2015, **78**, 246–263.
37 H. Tian, G. Guo, X. Fu, Y. Yao, L. Yuan and A. Xiang, *Int. J. Biol. Macromol.*, 2018, **120**, 475–490.
38 P. Lu, M. Guo, Y. Yang and M. Wu, *Polymers*, 2018, **10**, 1111.
39 N. T. Cervin, L. Andersson, J. B. S. Ng, P. Olin, L. Bergstrom and L. Wagberg, *Biomacromolecules*, 2013, **14**, 503–511.
40 M. Mihai, M. A. Huneault and B. D. Favis, *J. Appl. Polym. Sci.*, 2009, **113**, 2920–2932.
41 Z. Qu, D. Yin, H. Zhou, X. Wang and S. Zhao, *Eur. Polym. J.*, 2019, **116**, 291–301.
42 P. Ferkl, R. Pokorny, M. Bobak and J. Kosek, *Chem. Eng. Sci.*, 2013, **97**, 50–58.
43 A. Kaemmerlen, C. Vo, F. Asllanaj, G. Jeandel and D. Baillis, *J. Quant. Spectrosc. Radiat. Transfer*, 2010, **111**, 865–877.
44 A. Rizvi, R. K. M. Chu and C. B. Park, *ACS Appl. Mater. Interfaces*, 2018, **10**, 38410–38417.
45 F. Kreith, R. M. Manglik and M. S. Bohn, *Principles of heat transfer*, Cengage Learning, Stamford, CT, 7th edn, 2011.
46 M. Modest, *Radiative heat transfer*, Academic Press, Cambridge, MA, 2nd edn, 2003.
47 G. Wang, C. Wang, J. Zhao, G. Wang, C. B. Park and G. Zhao, *Nanoscale*, 2017, **9**, 5996–6009.
48 V. Bernardo, J. Martin-de-Leon, J. Pinto, R. Verdejo and M. A. Radriguez-Perez, *Polymer*, 2019, **160**, 126–137.
49 J. O. Akindoyo, M. D. H. Beg, S. Ghazali, M. R. Islam, N. Jeyaratnam and A. R. Yuvaraj, *R. Soc. Chem. Adv.*, 2016, **6**, 114453–114482.
50 M. Kirpluks, D. Kalnbunde, H. Benes and U. Cabulis, *Ind. Crops Prod.*, 2018, **122**, 627–636.
51 M. Desroches, M. Escouvois, R. Auvergne, S. Caillol and B. Boutevin, *Polym. Rev.*, 2012, **52**, 38–79.
52 N. N. Pauzi, R. Majid, M. H. Dzulkifli and M. Y. Yahya, *Composites, Part B*, 2014, **67**, 521–526.
53 S. Zhang, A. Xiang, H. Tian and A. V. Rajulu, *J. Polym. Environ.*, 2018, **26**, 15–22.
54 P. Furtwengler, R. M. Boumbimba and L. Averous, *Macromol. Mater. Eng.*, 2018, **303**, 1700501.
55 N. Ozveren and M. O. Seydibeyoglu, *Int. J. Polym. Sci.*, 2017, **2017**, 6310198.
56 H. Fan, A. Tekeei, G. J. Suppes and F.-H. Hsieh, *Int. J. Polym. Sci.*, 2012, **2012**, 474803.
57 ASTM D6400-19, *Standard Specification for Labeling of Plastics Designed to be Aerobically Composted in Municipal or Industrial Facilities*, ASTM International, West Conshohocken, PA, 2019.
58 M. Ghasemlou, F. Daver, E. P. Ivanova and B. Adhikari, *Eur. Polym. J.*, 2019, **118**, 668–684.
59 X. Xi, A. Pizzi, C. Geradin, H. Lei, X. Chen and S. Amirou, *Polymers*, 2019, **11**, 1802.
60 X. Xi, A. Pizzi, C. Geradin and G. Du, *J. Renewable Mater.*, 2019, **7**, 301–312.
61 Y. Chen, S. Yang, D. Fan, G. Li and S. Wang, *ACS Sustainable Chem. Eng.*, 2019, **7**, 12878–12886.
62 H. G. Kim, Y.-S. Kim, L. K. Kwac, H. J. Shin, S. O. Lee, U. S. Lee and H. K. Shin, *Nanomaterials*, 2019, **9**, 158.
63 R. Li, H. Lin, P. Lan, J. Gao, Y. Huang, Y. Wen and W. Yang, *Polymers*, 2018, **10**, 1319.
64 S. He, C. Liu, X. Chi, Y. Zhang, G. Yu, H. Wang, B. Li and H. Peng, *Chem. Eng. J.*, 2019, **371**, 34–42.
65 T. Rokkonen, H. Peltola and D. Sandquist, *J. Appl. Polym. Sci.*, 2019, **136**, 48202.
66 J. S. Colton and N. P. Suh, *Polym. Eng. Sci.*, 1987, **27**, 500–503.
67 J. S. Colton and N. P. Suh, *Polym. Eng. Sci.*, 1987, **27**, 485–492.
68 M. Stanzione, M. Oliviero, M. Cocca, M. E. Errico, G. Gentile, M. Avella, M. Lavorgna, G. G. Buonocore and L. Verdolotti, *Carbohydr. Polym.*, 2020, **231**, 115772.
69 M. Nofar and C. B. Park, *Prog. Polym. Sci.*, 2014, **39**, 1721–1741.
70 M. Nofar, D. Scligil, P. J. Carreau, M. R. Kamal and M.-C. Heuzey, *Int. J. Biol. Macromol.*, 2019, **125**, 307–360.
71 J. Ludwiczak and M. Kozlowski, *J. Polym. Environ.*, 2015, **23**, 137–142.
72 S. Li, G. He, X. Liao, C. B. Park, Q. Yang and G. Li, *RSC Adv.*, 2017, **7**, 6266–6277.
73 A. Ameli, D. Jahani, M. Nofar, P. U. Jung and C. B. Park, *Compos. Sci. Technol.*, 2014, **90**, 88–95.
74 T. Standau, C. Zhao, S. M. Castellon, C. Bonten and V. Altstadt, *Polymers*, 2019, **11**, 306.
75 J. Li, X. Liao, Q. Yang and G. Li, *Ind. Eng. Chem. Res.*, 2017, **56**, 11111–11124.
76 L. M. Matuana, O. Faruk and C. A. Diaz, *Bioresour. Technol.*, 2009, **100**, 5947–5954.
77 A. Kmetty, K. Litauszki and D. Reti, *Appl. Sci.*, 2018, **8**, 1960.
78 T. He, X. Liao, Y. He and G. Li, *Prog. Nat. Sci.: Mater. Int.*, 2013, **23**, 395–401.
79 S. Mali, F. Debiagi, M. V. E. Grossmann and F. Yamashita, *Ind. Crops Prod.*, 2010, **32**, 353–359.
80 I. Mariam, K. Y. Cho and S. S. H. Rizvi, *Int. J. Food Prop.*, 2008, **11**, 415–426.
81 A. E. S. Vercelheze, F. M. Fakhouri, L. H. Dall'Antonia, A. Urbano, E. Y. Youssef, F. Yamashita and S. Mali, *Carbohydr. Polym.*, 2012, **87**, 1302–1319.
82 S. Ketkaew, P. Kasemsiri, S. Hiziroglu, W. Mongkolthanaruk and R. Wannasutta, *J. Polym. Environ.*, 2018, **26**, 311–318.
83 J. B. Engel, A. Ambrosi and I. C. Tessaro, *Carbohydr. Polym.*, 2019, **225**, 115234.
84 C. Rojas, M. Cea, A. Iriarte, G. Valdes, R. Navia and J. P. Cardenas-R, *Sustainable Mater. Technol.*, 2019, **20**, e00102.
85 D. Liu, H. Tian and L. Zhang, *J. Appl. Polym. Sci.*, 2007, **106**, 130–137.

86 H. Tian, D. Liu and L. Zhang, *J. Appl. Polym. Sci.*, 2009, **111**, 1549–1556.
87 P. Chen, H. Tian, L. Zhang and P. R. Chang, *Ind. Eng. Chem. Res.*, 2008, **47**, 9389–9395.
88 G. Guo, C. Zhang, Z. Du, W. Zou and H. Li, *J. Polym. Environ.*, 2015, **23**, 183–189.
89 B. Liu, L. Jiang and J. Zhang, *Macromol. Mater. Eng.*, 2011, **296**, 835–842.
90 Z. Chen, J. Hu, J. Ju and T. Kuang, *Polymers*, 2019, **11**, 1852.
91 S. C. Frerich, *J. Supercrit. Fluids*, 2015, **96**, 349–358.
92 K. Ru, S. Zhang, X. Peng, J. Wang and H. Peng, *Polymer*, 2019, **185**, 121967.
93 Y. Zhang, B. Lu, F. Lv, W. Guo, J. Ji, P. K. Chu and C. Zhang, *J. Appl. Polym. Sci.*, 2012, **126**, 756–761.
94 J.-F. Yue, L. Gan, C.-H. Liu, X.-Z. Ma, D. Wang and J. Huang, *Polymer*, 2018, **155**, 50–57.
95 A.-K. Lim, S.-G. Jang, S.-I. Lee, K.-H. Lee and I.-J. Chin, *Macromol. Res.*, 2008, **16**, 218–223.
96 S. Bonham and M. Misra, *Macromol. Mater. Eng.*, 2011, **296**, 788–801.
97 J. Zhou, Z. Yao, C. Zhou, D. Wei and S. Li, *J. Appl. Polym. Sci.*, 2014, **131**(18), 40773.
98 H. Ventrua, L. Sorrentino, E. Languna-Gutierrez, M. A. Rodriguez-Perez and M. Ardanuy, *Polymers*, 2018, **10**, 249.
99 D. M. Panaitescu, R. Trusca, A. R. Gabor, C. A. Nicolae and A. Casarica, *Int. J. Biol. Macromol.*, 2020, **164**, 1867–1878.
100 R. E. Lee, T. Azdast, G. Wang, X. Wang, P. C. Lee and C. B. Park, *Int. J. Biol. Macromol.*, 2020, **155**, 286–292.
101 D.-D. Ye, T. Wang, W. Liao, H. Wang, H.-B. Zhao, Y.-T. Wang, S. Xu and Y.-Z. Wang, *ACS Sustainable Chem. Eng.*, 2019, **7**, 11582–11592.
102 A. Fraleoni-Morgera and M. Chhikara, *Adv. Eng. Mater.*, 2019, **21**(7), 1801162.
103 F. A. Govan, D. M. Greason and J. D. McAllister, *Thermal insulation, materials, and systems for energy conservation in the 80's*, ASTM International, West Conshohocken, PA, 1983.
104 B. Notario, J. Pinto, E. Solorzano, J. A. de Saja, M. Dumon and M. A. Rodriguez-Perez, *Polymer*, 2015, **56**, 57–67.
105 X. Lu, R. Caps, J. Fricke, C. T. Alviso and R. W. Pekala, *J. Non-Cryst. Solids*, 1995, **188**, 226–234.
106 R. J. J. Williams and C. M. Aldao, *Polym. Eng. Sci.*, 1983, **23**, 293–298.
107 Z. M. Zhang, *Nano/Microscale Heat Transfer*, McGraw-Hill Education, NY, 1st edn, 2007.
108 J. Lee, J. Lim and P. Yang, *Nano Lett.*, 2015, **15**, 3273–3279.
109 X. Lu, M. C. Arduini-Schuster, J. Kuhn, O. Nilsson, J. Fricke and R. W. Pekala, *Science*, 1992, **255**, 971–972.
110 M. G. Ghossoub, K. V. Valavala, M. Seong, B. Azerdo, K. Hsu, J. S. Sadhu, P. K. Singh and S. Sinha, *Nano Lett.*, 2013, **13**, 1564–1571.
111 H. Malekpour, P. Ramnani, S. Srinivasan, G. Balasubramanian, D. L. Nika, A. Mulchandani, R. K. Lake and A. A. Balandin, *Nanoscale*, 2016, **8**, 14608–14616.
112 H. Ma and Z. Tian, *Appl. Phys. Lett.*, 2015, **107**, 073111.
113 G. F. Smits, *J. Therm. Insul. Build. Envelopes*, 1994, **17**, 309–329.
114 D. M. Bigg, in *Thermal and Electrical Conductivity of Polymer Materials*, Springer, Berlin, Heidelberg, 1995, vol. 119, pp pp. 1–30.
115 Z. Han and A. Fina, *Prog. Polym. Sci.*, 2011, **36**, 914–944.
116 W. Van De Walle, S. Claes and H. Janssen, *Constr. Build. Mater.*, 2018, **182**, 427–440.
117 W. Van De Walle and H. Janssen, *J. Build. Phys.*, 2019, **43**, 277–300.
118 M. Wang, J. Wang, N. Pan and S. Chen, *Phys. Rev. E: Stat., Nonlinear, Soft Matter Phys.*, 2007, **75**, 036702.
119 W. She, Y. Zhang and M. R. Jones, *Constr. Build. Mater.*, 2014, **50**, 421–431.
120 J. Randrianalisoa, D. Baillis, C. L. Martin and R. Dendievel, *Int. J. Therm. Sci.*, 2015, **98**, 277–286.
121 G. Gaiselmann, M. Neumann, V. Schmidt, O. Pecho, T. Hocker and L. Holzer, *AIChE J.*, 2014, **60**, 1983–1999.
122 R. Hasanzadeh, T. Azdast, A. Doniavi and M. Rostami, *Heat and Mass Transfer*, 2019, **55**, 2845–2855.
123 Y. Li, J. Mi, H. Fu, H. Zhou and X. Wang, *ACS Omega*, 2019, **4**, 12512–12523.
124 E. Cuce, P. M. Cuce, C. J. Wood and S. B. Riffat, *Renewable Sustainable Energy Rev.*, 2014, **34**, 273–299.
125 *Engineering ToolBox, Thermal Conductivity of selected Materials and Gases*, https://www.engineeringtoolbox.com/thermal-conductivity-d_429.html, accessed, 25 June, 2020.
126 L. V. Nielsen, H.-P. Ebert, F. Hemberger, J. Fricke, A. Biedermann, M. Reichelt and U. Rotermund, *High Temp. – High Pressures*, 2000, **32**, 701–707.
127 R. Guo, Z. Ren, H. Bi, M. Xu and L. Cai, *Polymers*, 2019, **11**, 549.
128 *National Center for Biotechnology Information, Cellulose*, https://pubchem.ncbi.nlm.nih.gov/compound/CELLULOSE#section=Density, https://pubs.acs.org/doi/10.1021/acsami.8b22134, accessed, June 25, 2020.
129 *Ingeo™ Biopolymer 8052D Technical Data Sheet*, https://www.natureworksllc.com/~/media/Files/NatureWorks/Technical-Documents/Technical-Data-Sheets/TechnicalDataSheet_8052D_foam_pdf.pdf?la=en, accessed Dec 22, 2020.
130 D.-c. Li, T. Liu, L. Zhao, X.-s. Lian and W.-k. Yuan, *Ind. Eng. Chem. Res.*, 2011, **50**, 1997–2007.
131 N. Najafi, M.-C. Heuzey, P. J. Carreau, D. Therriault and C. B. Park, *Eur. Polym. J.*, 2015, **73**, 455–465.
132 J. Li, G. He, X. Liao, Q. Yang and G. Li, *RSC Adv.*, 2015, **5**, 36320–36324.
133 P. Bhati and N. Bhatnagar, *Mater. Lett.*, 2017, **209**, 602–605.